THESIS FOR THE DEGREE OF LICENTIATE OF ENGINEERING

Solids flows in circulating fluidized beds: explorations of phenomena with applications to boilers

TOVE DJERF

Department of Space, Earth and Environment

CHALMERS UNIVERSITY OF TECHNOLOGY

Gothenburg, Sweden 2020

Solids flows in circulating fluidized beds: explorations of phenomena with applications to boilers

TOVE DJERF

Department of Space, Earth and Environment
Chalmers University of Technology
SE-412 96 Gothenburg
Sweden
Telephone + 46 (0)31-772 1000

Cover:
[Fluid-dynamical scaling with Glicksman simplified scaling laws,
between small cold laboratory unit and large hot CFB boiler,
se section 2.2 for further details.
- CFB boiler figure with permission from Valmet Technologies Oy]

Printed by Chalmers Digitaltryck
Chalmers University of Technology
Gothenburg, Sweden 2020

Solids flows in circulating fluidized beds: explorations of phenomena with applications to boilers

TOVE DJERF
Division of Energy Technology
Department of Space, Earth and Environment
Chalmers University of Technology

Abstract

The circulating fluidized bed (CFB), which is a technology that is commonly used in the heat and power sector, efficiently converts renewable and/or and low-grade solid fuels, such as biomass and biogenic waste fractions. CFB units serve also as a technological platform for carbon capture processes (combustion by oxy-firing or chemical looping), which are foreseen to play a key role in the transition of the energy system towards decreased atmospheric CO_2 emissions. However, the development of commercial CFB boilers is limited by key gaps in the knowledge, one of which is the solids flow pattern, which is not sufficiently understood even though it is an important phenomenon that governs both mass and heat transfers in the system.

This thesis aims to elucidate the solids flow patterns in CFB units that are representative of large-scale boilers. More specifically, the objectives are to identify and characterize the interlinked underlying phenomena that govern the solids flow pattern in the riser and the external circulation of solids. The specific phenomena studied here are: depletion of the dense bed; solids entrainment from the bottom region; the back-mixing in the splash and transport zones; and the riser exit backflow. Also examined is how these factors are affected by the unit size. For these purposes we conducted experimental analyses in two units: a pseudo-2-dimensional unit; and a fluid-dynamically down-scaled unit (in which studies were carried out with and without scaled bed material). Validation of the cold-flow scale model with scaled material shows very good similarity between the concentration profiles obtained from the cold-flow scale model and from the large-scale (>200-MW_{th}) CFB reference boiler.

The results show that the presence/absence of a dense bed affects the entrainment of particles from the bottom region into the freeboard. The expansion of the splash zone immediately above the dense bed is affected by the dense bed height due to the modified bubble growth. The solids back-mixing from the core region to the wall layers is mostly affected by the gas velocity and the cross-sectional geometry of the riser. Finally, the external circulation of solids is shown to be non-equal the upwards solids flux at the top of the riser, with the exceptions of cases with very low gas velocities, revealing significant local back-mixing of solids at the furnace exit at nominal loads.

Keywords: fluidization, circulating fluidized bed boiler, solids flow, fluid dynamics, scaling

List of Publications

This thesis is based on the following papers, which are referred to in the thesis according to their Roman numerals:

I. T. Karlsson, X. Liu, D. Pallarès. F. Johnsson
Solids circulation in circulating fluidized beds with low riser aspect ratio and varying total solids inventory.
Powder Technology 316 (2017): 670–676.

II. T. Djerf, D. Pallarès. F. Johnsson
Bottom-bed fluid dynamics–Influence on solids entrainment.
Fuel Processing Technology 173 (2018): 112–118.

III. T. Djerf, D. Pallarès. F. Johnsson
Solids flow pattern in large-scale CFB boilers: experimental evaluation at fluid-dynamical downscaled conditions.
Submitted for publication (Autumn 2020)

Tove Djerf (–formerly, Karlsson) is the main researcher in all the papers. Associate Professor David Pallarès and Professor Filip Johnsson have contributed with guidance in the experimental work, discussions, writing and editing of the papers. Dr. Xuemin Lui from Tsinghua University has contributed with experimental work to **Paper I**.

Table of Contents

To my Family

"Take a deep breath,
pick yourself up,
dust yourself off,
and start all over again"

– *Dorothy Fields (1936), Nat King Cole (1944), Frank Sinatra (1962)*

1. Introduction

Mitigation of climate change and the continuing search for a reliable energy supply drive technical developments in the heat and power sector. The need for such developments is made clear in the Summary Insight of 2016 from the IEA, which lists higher efficiency, a larger share of renewables, and significant use of carbon capture and storage (CCS) among the pathways to meet the goals set out in the Paris Agreement [1]. Thus, the future for fossil fuel combustion is framed only within the context of the CCS technology. Several carbon capture technologies have been developed, and those that are proposed to play a significant role in the future energy system are oxyfuel combustion, chemical looping combustion, and post-combustion capture. However, there are disadvantages associated with these technologies, including increased capital and operational costs and decreased plant efficiencies. Regarding renewable fuels, although an increase in the general use of biomass is envisioned as a pathway to decreased CO_2 emissions, the heat and power sector will need to compete with other sectors for the available biomass feedstock [2]. It is likely that this competition will limit the future pool of renewable fuel options for the heat and power sector to various types of available low-grade biomass and biogenic waste fractions. These fuels are problematic in terms of issues with agglomeration, slag formation, corrosion, and NO_x formation during combustion to name a few, and they require highly advanced technologies for smooth usage. In addition, the units that will be used for converting biogenic fuels are expected to be small in size, as it is not economically feasible to transport over long distances feedstocks of low energy density. Such smaller boilers tend to exhibit lower combustion efficiencies, due to shorter gas residence times and increased char losses, and this represents one of the main challenges for using units with low-grade fuels [3]. Finally, the increase in non-dispatchable renewable energy in the forms of wind and solar power means that there will be a general need for dispatchable energy to operate efficiently at different load levels and to transition smoothly between these load levels.

Considering the above, the fluidized bed (FB) technology – commonly used for the thermochemical conversion (combustion, gasification and pyrolysis) of solid fuels – is foreseen as an important technology in the future energy system, due to its high fuel flexibility and in-bed emissions control through the use of active bed materials [3-5]. Initially, fluidized bed boilers were designed to operate at gas velocities below the terminal velocity of the bed material (i.e., without significant entrainment of the bed material), in so-called bubbling fluidized beds (BFB). Owing to their investment costs, such BFB units have been commercially operated at scales typically above 30 MW_{th} [4]. For improved economy and performance at larger scales, an increase in the specific thermal effect (MW/m^2) was achieved through the use of higher gas velocities. As this entailed significant entrainment of the bed material from the bottom region of the boiler, a solids recirculation system had to be implemented, resulting in so-called circulating fluidized bed (CFB) units. CFB boilers imply a higher investment cost than BFBs and are typically commercialized

for boiler scales >100 MW_{th} (typically in combined heat and power or heat-only boiler schemes) and up to around 1,400 MW_{th} (in power boilers, with outputs of around 550 MW_e). Such CFB units are characterized by good gas-solids contacts and relatively high thermal mixing and inertia, providing fields of temperature and heat extraction.

Given the above characteristics, the CFB technology can contribute to the future energy system through:

- The implementation of dual fluidized bed systems for
  - chemical looping combustion for carbon capture [6]
  - indirect gasification to produce high-quality biogas [7]
  - calcium looping for carbon capture [8]
- The use of active bed material for
  - improved conversion of low-grade fuels, e.g., oxygen carrier-aided combustion [9]
  - thermochemical energy storage processes [10]
- The application of compact designs for oxyfuel furnaces for carbon capture [11] [12]

Even if the CFB technology is a key component of these applications, there is a general scarcity of knowledge regarding the solids flow and mixing patterns within the different CFB reactor applications. Acquisition of this knowledge is crucial for enabling reliable scale-up and design of the reactor systems, since they govern mass and heat transport within the CFB reactors. Thus, it is important to understand the underlying phenomena that govern the solids flow pattern in the riser and the external circulation of solids. Since most of the experimental work is typically carried out under ambient conditions at small scales, in order to provide access for measurements and limit costs, it is also important to know the influence of the size of the unit and how the phenomena can be scaled.

An understanding of the phenomena governing the flow of solids in a CFB reactor could theoretically be achieved by modeling the CFB gas-solids flow from first principles, i.e., computational fluid-dynamics (CFD). However, this is not really feasible because it either requires excessive computational effort (for the Lagrangian description of each solid particle) or contains too-uncertain formulations for some terms in the governing equations (for the Eulerian description of the solids phase as a continuum) [13]. Instead, semi-empirical modeling is being used increasingly in the development of the CFB technology. In this type of modeling, knowledge of the CFB is based on experimental data (see [14-22]) and is used to formulate hypotheses for the macroscopic solids flow [23-26], instead of solving the momentum equations for the solids and gas phases.

1.1 Aim and Scope

The aim of the work presented in this thesis is to extend our current knowledge of the solids flow pattern in CFB units that are representative of CFB boilers, which is the application in focus. Moreover, the insights gained from this work should contribute to a more general understanding of other CFB reactor applications, as mentioned above. More specifically,

this work aims to discover what is governing the CFB solids flow pattern, with the objective of identifying and characterizing the interlinked underlying phenomena governing the solids flow pattern in the riser and the external circulation of solids. The specific phenomena studied here are: the dense bed depletion; solids entrainment from the bottom region; the back-mixing in the splash and transport zones; and the riser exit backflow. How these elements act together to yield the external circulation of solids, and whether the unit size affects the different phenomena are issues that are addressed in this thesis. The in-depth knowledge gained from these investigations is expected to contribute to CFB development, not only by virtue of its inherent value, but also by yielding refined assumptions regarding the solids flow pattern for semi-empirical models and high-quality experimental data for validation of CFD modeling.

The scope of the work is restricted to geometries and conditions relevant to large-scale CFB boilers. The characteristics of such units are: solids in the Geldart group B; geometries with a furnace aspect ratio in the order of 10 or less; operation yielding a bed aspect ratio of less than 1 (resulting in non-slugging conditions); and an external circulation of solids <20 kg/m^{2}s.

1.2 Methodology

Semi-empirical modeling presents an obvious challenge in terms of formulating general hypotheses that are valid for wide ranges of sizes and operational conditions, as opposed to describing a specific operational interval in a particular unit. Thus, validation of the hypotheses taken for wide ranges of unit sizes and operational conditions is of critical importance and depends directly on the availability of such experimental data. However, as *in situ* measurements are difficult to perform, and since the available measurement data are of poor resolution and limited to a certain operational range in active CFB boilers, and the large CFB boiler technology is subject to secrecy policies, very few datasets from real CFB boilers have been published. This has resulted in a knowledge gap, and one solution to this is the use of fluid-dynamically down-scaled cold-flow models to generate the required experimental data on the solids flow patterns.

In order to achieve the aim of this thesis, experimental analysis of the solids flow is conducted in two different units operated under ambient conditions: a pseudo-2-dimensional CFB unit; and a cold-flow model. The latter is fluid-dynamically down-scaled from an existing large-scale CFB boiler, operated in two separate studies with non-scaled bed materials and scaled bed materials, respectively. The fluid-dynamic down-scaling is validated against measurements made in a 200-MW$_{th}$ reference CFB boiler, and the results obtained from test campaigns are compared with the values published in the literature. The measuring techniques used are pressure sampling (*via* piezoelectric transducers) and evaluation of the external circulation of solids (using an in-house method that involves a specially designed fluidizing valve).

1.3 Outline of the papers

- **Paper I** provides an overview of the solids flow phenomena in the riser of a CFB riser. The analysis of the results is limited to a qualitative framework, since a pseudo-2-dimensional unit is used.
- **Paper II** presents the first results obtained from the dedicated 3-dimensional unit that was designed and built for the work of this thesis. The unit is dimensioned according to scaling laws. However, this work uses non-scaled bed material, to allow us to become acquainted with the unit and to study the fluid dynamics of solids with less-challenging handling.
- **Paper III** studies the solids flow established in the fluid-dynamically down-scaled cold-flow model when it is operated with flows and bed material according to scaling laws, such that it resembles the reference large-scale boiler. This provides values representative of commercial CFB boilers and, therefore, results with quantitative relevance.

2. Theory

2.1 Solids flow patterns in CFB boilers

The solids flow pattern in fluidized beds has been studied extensively for many years. The fluidized bed that is representative of CFB boilers typically contains a bottom dense bed with gas bubbles, which through their eruption at the dense bed surface entrain material upwards in the freeboard [27]. Kunii and Levenspiel [28] have described the entrainment of solids from the dense bed in terms of a solids phase flowing upwards as it back-mixes, whereby eruptions of the bubbles eject agglomerates of particles into the freeboard. Thus, the particles either fall back down onto the dense bed surface – generating the so-called splash zone - or they are effectively entrained from the bottom region as a dispersed phase [28]. These disperse, entrained solids flow upwards as a core flow, given that they partially back-mix along the furnace by entering the down-flowing solids wall layers formed by the furnace walls [17]. Once they arrive at the riser exit, the solids can be internally circulated into the wall layers through back-flow or they are externally recirculated through the cyclone and seal system, eventually being returned into the bottom of the riser [14, 20, 28-30].

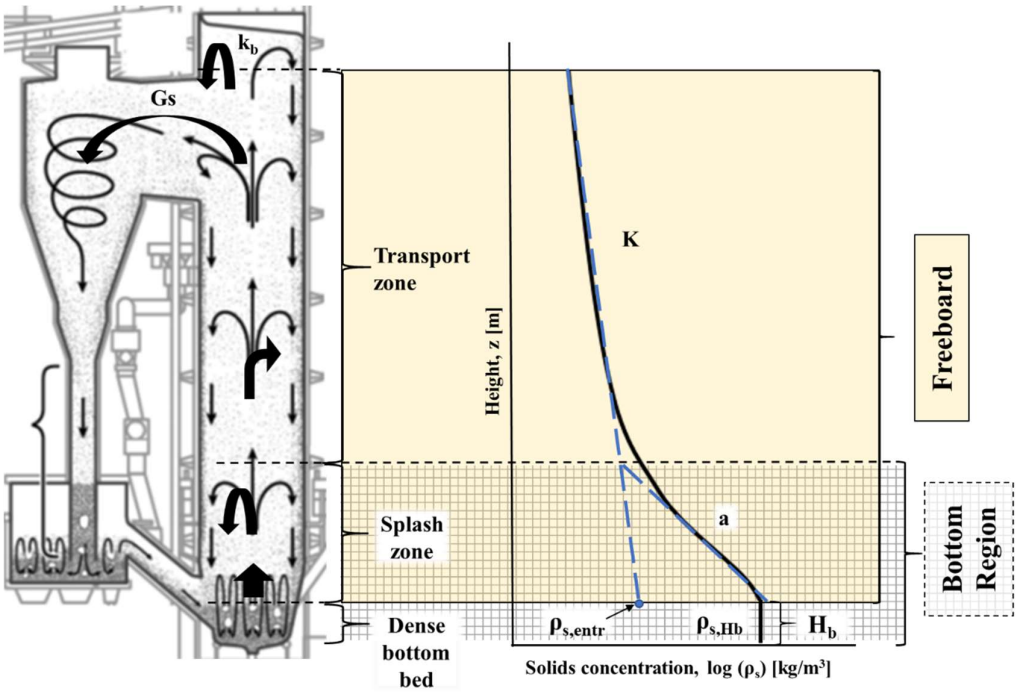

Figure 1. Fluid-dynamical regions in the riser of a CFB boiler according to Johnsson and Leckner [14], including a typical vertical profile of solids concentration and the key parameters used in the mathematical descriptions in Eqs. (5.1) and (5.2).

Figure 1 depicts the three different fluid-dynamical zones in a CFB boiler [14], with the bottom region consisting of the dense bottom bed directly above the distributor plate and the splash zone. The latter, together with the transport zone occupied by the disperse phase form the so-called 'freeboard'.

Dense bed

Even though the fluidization velocity exceeds the terminal velocity of the particles in a CFB boiler, a dense bottom region similar to a bubbling bed was identified in the 12-MW_{th} Chalmers boiler [31]. This was attributed to the strong local fluctuations in gas velocity caused by the limited pressure drop across the distributor plate, which is typically applied in CFB boilers to decrease the costs of the fans. Thus, the dense bed contains bubbles of the exploding type [32] and shows a constant time-averaged solids concentration over its height, yielding a linear pressure drop with height. The height of the dense bed is dependent upon the amount of bed material in the CFB loop and the fluidization velocity applied [33]. When combinations of sufficiently high fluidization velocities and sufficiently low solids inventories are applied, the dense bed is depleted.

Splash zone

Above the dense bed, a splash zone develops as bubble eruptions at the dense bed surface eject clustered solids into the freeboard. The strong solids back-mixing follows a ballistic pattern and results in a steep decrease in the solids concentration with height, which can be described by an exponential decay coefficient, *a* [14, 34], in this commonly used formulation for BFB and CFB boilers;

$$\rho_{cluster}(h) = \rho_{cluster}]_{H_b} \; e^{-a(h-H_b)} \tag{1}$$

where the decay constant is often described [35-40] as:

$$a \propto \frac{u_g}{u_t} \tag{2}$$

Transport zone

Above the splash zone, CFB boilers exhibit a transport zone that occupies most of the riser height and is populated by solids entrained from the bottom region (the dense bed and the splash zone). The solids back-mixing, which consists of a net lateral flow from the upwards core flux to the downwards wall layers, can be described by a decay coefficient, *K* [14], in the concentration description of the transport zone;

$$\rho_{disperse}(h) = \rho_{disperse}\Big]_{H_b} \; e^{-K(h-H_b)} \tag{3}$$

where the decay constant that is often used [35-39, 41, 42] has the following form [14]:

$$K \propto \frac{1}{u_g - u_t} \tag{4}$$

Combining the concentration description of the dense bed, the splash zone [Eq. (1)], and the transport zone [Eq. (3)] generates a general expression for the vertical profile of solids concentration in the riser of a CFB furnace exemplified in Figure 1:

$$\rho_s(h) = \rho_{s,H_b} \qquad h < H_b \tag{5.1}$$

$$\rho_s(h) = \left(\rho_{s,H_b} - \rho_{s,entr}\right)e^{-a(h-H_b)} + \rho_{s,entr}e^{-K(h-H_b)} \qquad h > H_b \tag{5.2}$$

where $\rho_{s,entr}$ is the concentration of effectively entrained solids from the bottom bed (see Figure 1). This value is obtained from the extrapolation of the upper concentration profile to the dense bed height, H_b (or in the absence of a dense bed, down to the bottom grid) (see Figure 1) [43, 44]. Various expressions for ρ_{s,H_b}, [37, 40], a [14, 34] and K [14, 30] are listed in the literature. However, the effective solids entrainment from the bottom region (here characterized by $\rho_{s,entr}$) for CFB boiler conditions remains unstudied.

The external circulation of solids is often estimated to be equal to the solids up-flow at the riser top [14, 15, 35, 45, 46]. However, studies have shown that there can be significant solids back-mixing at the riser exit (known as the 'back-flow effect') [35, 37, 47-49]. The back-flow ratio, k_b, is defined as:

$$k_b = \frac{G_{s,layer}}{G_{s,core}}\bigg|_{furnace\ top} \tag{6}$$

The back-flow has been shown to depend on the geometry of the exit region [29, 47, 48], as well as the local particle size and concentration [37].

External circulation

External circulation of solids in a CFB boiler eventually results from a sequence of fluid-dynamical mechanisms that entails solids entrainment from the bottom region, solids back-mixing in the transport zone and, finally, back-mixing in the exit region. These processes are characterized by the terms $\rho_{s,entr}$, K and k_b, respectively, and can be aggregated to yield the externally circulating solids flux:

$$G_s = \underbrace{\rho_{s,entr}\left(u_g - u_t\right)}_{\text{entrained from bottom region}}\ \underbrace{e^{-K(H_{TOP}-H_b)}\ (1-k_b)}_{\text{yielding furnace top}} \tag{7}$$

Measurement of the external circulation of solids in large-scale units is a major challenge. Only a few values are published in the literature [15, 20, 45, 46, 50], and some of these lack a clear description of their calculation. For this, a consistent, well-documented method is by solving the heat balance over a loop seal system equipped with a heat exchanger [46]. In addition, care should be taken when comparing values for the external solids circulation obtained from different units, since several unit-specific variables (e.g., riser height, cross-sectional dimensions, secondary air location, and tapered walls inclination) are known to influence the external solids circulation.

2.2 Fluid-dynamical scaling

Fluid-dynamical scaling is used in many different applications because it facilitates studies of the fluid dynamics of challenging environments (e.g., large-scale, industrial environments, high-temperature conditions) in smaller laboratory units operated under ambient conditions, without losing the quantitative relevance of the measured data. Fluid-dynamical scaling also allows the use of diagnostic techniques that are not suitable for harsh environments. Fluid-dynamical scaling is based on the reformulation of continuity and momentum balances into their dimensionless forms and, from that, extraction of the dimensionless parameters that need to be held constant in order to maintain similarity between the reference and the laboratory unit. Table 1 shows the collected scaling parameters for the different scaling sets discussed below, together with their respective positive and negative aspects.

Glicksman [51] proposed a full set of scaling parameters for a fluidized bed (used, for example, in [52, 53]). See row 1 in Table 1, in which the length scale factor, L^*, is given by the gas chosen for operation of the cold-flow model:

$$\frac{u_0^2}{gD}, \frac{\rho_p}{\rho_g}, \frac{\rho_p u_0 d_p}{\mu_f}, \frac{\rho_f u_0 L}{\mu_f}, \frac{L}{D}, \frac{G_s}{\rho_p u_0}, \emptyset, PSD \tag{8.1}$$

$$L^* = \frac{L_{cold}}{L_{hot}} = \left(\frac{\mu_f}{\rho_f}\Big]_{cold} \Big/ \frac{\mu_f}{\rho_f}\Big]_{hot} \right)^{2/3} \tag{8.2}$$

When applied to the down-scaling of a CFB combustor (operating at approximately 850°C) to a cold-flow model fluidized with ambient air, Eq. (8.2) yields a length scale factor of around L^*=0.2. Note that for utility-scale CFB boilers (with riser heights typically up to 40 m), this would imply air-blown cold-flow models of considerable dimensions (8 m in height).

Both Horio et al. [54] and Glicksman et al. [55] have presented simplified scaling laws, in rows 3 and 2, respectively, in Table 1, where Glickman's simplified set of scaling reads:

$$\frac{u_0^2}{gD}, \frac{\rho_p}{\rho_g}, \frac{u_0}{u_{mf}}, \frac{L}{D}, \frac{G_s}{\rho_p u_0}, \emptyset, PSD \tag{9.1}$$

The set of scaling laws presented by Horio and colleagues is similar, with u_t substituting for u_{mf} in the third dimensionless group [56]. This results in only minor variations of the resulting scaling.

The simplified set of scaling laws results in a length scale factor of:

$$L^* = \frac{L_{cold}}{L_{hot}} = \left(\frac{u_{mf}]_{cold}}{u_{mf}]_{hot}} \right)^2 \tag{9.2}$$

This length scale factor can be adjusted by varying the particle size [note that the solids density is given by the second dimensionless group in Eq. (8.1) or Eq. (9.1)], resulting in finer solids yielding smaller cold-flow models. It should also be noted that for finer solids, other forces may also affect the solids flow, e.g., inter-particle forces and static charging. Therefore, it is crucial to keep the scaled solids in the same Geldart group as the reference solids. The flexibility

offered by the simplified set in designing cold-flow models has meant that it has evolved into a widely used tool in the field of fluidization (see for example [29, 48, 55-59]). The validity of this simplified set of scaling laws is proven at both low and high particle Reynolds numbers, i.e., it is assumed to be generally valid.

Hazardous material and environmental issues arise with very small and heavy particles. Van der Meer et al. [56] have proposed a further simplification of the scaling sets (see row 4 in Table 1), whereby the $\frac{\rho_p}{\rho_g}$ parameter is omitted [56], providing the opportunity to choose the particles more freely. This has been validated experimentally by Glicksman for very low Reynolds numbers [60]. Van der Meer et al. [56] have noted that this simplified scaling maintains only approximately the fluidization regime and macroscopic movement of the solids. The mass and pressure drop similarities are lost, while the riser solids volumetric hold-up is more or less maintained [56].

Table 1. Different sets of fluid-dynamical scaling laws and their negative and positive aspects.

Sets of fluid-dynamical scaling									**Negative aspects**	**Positive aspects**
Glicksman full set	$\frac{u_0^2}{gD}$	$\frac{\rho_p}{\rho_g}$	$\frac{\rho_p u_0 d_p}{\mu_f}$	$\frac{\rho_f u_0 L}{\mu_f}$	$\frac{L}{D}$	$\frac{G_s}{\rho_p u_0}$	$\emptyset$	PSD	Fixed-length scale factor. Yields fine, heavy particles in small units, and thus potentially strong inter-particle forces.	The fluid dynamics are fully scaled
Glicksman simplified set	$\frac{u_0^2}{gD}$	$\frac{\rho_p}{\rho_g}$	$\frac{u_0}{u_{mf}}$		$\frac{L}{D}$	$\frac{G_s}{\rho_p u_0}$	$\emptyset$	PSD	Yields fine, heavy particles in small units, and thus potentially strong inter-particle forces. Is associated with substantial challenges, e.g., hazardous properties.	Adjustable length scale factor. Validated for high and low particle Reynolds numbers.
Horio simplified set	$\frac{u_0^2}{gD}$	$\frac{\rho_p}{\rho_g}$	$\frac{u_0}{u_t}$		-	$\frac{G_s}{\rho_p u_0}$	-	-		
Van der Meer et al. simplified set	$\frac{u_0^2}{gD}$	-	$\frac{u_0}{u_t}$		$\frac{L}{D}$	$\frac{G_s}{\rho_p u_0}$	-	-	Loss of quantitative value for pressures/solids concentrations. Validated only for a viscous regime.	Adjustable length scale factor and solids type

In contrast to other CFB systems (e.g., fluid catalytic cracking), the external solids circulation in CFB boilers is not an externally controllable or a known parameter. Instead, it is a consequence of the riser design and operation. Thus, the dimensionless group $\frac{G_s}{\rho_p u_0}$ is dropped in the scaling of CFB boilers. Instead, the dimensionless riser pressure drop, $\Delta p/\rho_p g L$, must be accounted for to ensure similarity of the solids flows.

2.2.1 Down-scaling of a 200-MW_{th} CFB Boiler

In the present work, a reference 200-MW_{th} CFB boiler is fluid-dynamically down-scaled. The reference boiler has a cross-sectional area of 75 m^2 and a height of 40 m and is operated at

850°C with a bed material that consists primarily of make-up material (silica sand), with a mean particle diameter of 190 μm and a density of 2,600 kg/m^3.

Using Glicksman's full set of scaling laws and ambient air as the fluidization medium in the cold-scale model, the resulting scaling factor is L*=1/4.4=0.23. With this, the resulting cold-scale model would yield a height of 9.5 m and a cross-sectional area of 4.3 m^2 – requiring a ceiling height and air feeding capacity beyond what is affordable in our laboratory facilities. This case is marked in gray in Table 2, and would have been the optimal scaling. In Table 2, the values of the dimensionless groups applied in the scale model can be found in the last two columns, using two different sets of simplified scaling laws (Glicksman and van der Meer, respectively; *cf.* Table 1).

Table 2. Fluid-dynamical scaling discussed in this work. Up-scaled values for the corresponding boiler are given in parentheses.

			Reference Boiler	***Glicksman's full set*** *(not applied in this work)*	***Glicksman's simplified set*** *(applied in Paper III)*		***van der Meer's simplified set*** *(applied in thesis, based on results from Paper II)*
Cross-sectional area	$D \times W$	m^2	75	4.3 *(75)*	0.445 *(75)*		0.445 *(2.1)*
Height	L	m	40	**9.5** *(40)*	3.1 *(40)*		3.1 *(6.7)*
Gas density	ρ_g	kg/m^3	0.33	1.2 *(0.33)*	1.2 *(0.33)*		1.2 *(0.33)*
Gas viscosity	μ_g	Pas	4.3*10^{-5}	1.8*10^{-5} *(4.3*10^{-5})*	1.8*10^{-5} *(23*10^{-5})*		1.8*10^{-5} *(1.6*10^{-5})*
Particle diameter	d_p	μm	190	**45** *(190)*	35 *(194)*		112 *(382)*
Particle density	ρ_p	kg/m^3	2,600	**9,397** *(2,600)*	8,920 *(2,468)*		2,600 *(719)*
Minimum fluidization velocity	u_{mf}	m/s	0.0155	0.0076 *(0.0155)*	0.0043 *(0.0155)*		0.0127 *(0.019)*
Terminal velocity	u_t	m/s	0.95	0.46 *(0.96)*	0.28 *(1.01)*		0.64 *(0.95)*
Dimensional scaling factors (cold-flow model / reference unit)							
Length	$L^* = L_{Cold}/L_{Hot} = \left(u_{mf_{Cold}}/u_{mf_{Hot}}\right)^2$			0.23	0.077		0.45
Time	$t^* = t_{Cold}/t_{Hot} = \left(u_{0_{Cold}}/u_{0_{Hot}}\right)^2$			0.48	0.28		0.67
Mass	$m^* = m_{Cold}/m_{Hot} = \rho_{g_{Cold}}/\rho_{g_{Hot}} * (L_{Cold}/L_{Hot})^3$			0.0442	0.0016		0.340

Applying Glicksman's simplified set of scaling laws, a scale model that operates with ambient air can be designed that offers a somewhat adjustable scaling (see Section 2.2) through the choice of solids. A good compromise was judged to be a length scale factor of 1/13, which requires solids that yield a minimum fluidization velocity of 0.0043 m/s [Eq. (9.2)] in the cold-scale model. The optimal solids density (9,397 kg/m^3) is given by the density ratio, although materials with this density value present substantial challenges in that they can be: hazardous (lead mixtures), especially at the fine sizes required (30–50 μm); radioactive (polonium); or very expensive (silver mixtures). As a consequence, copper (8,920 kg/m^3) was chosen as the bed material for the cold-scale model. With the solids density fixed, the solids size is the parameter through which the minimum fluidization velocity (and thereby the length scale factor) can be adjusted. The design values for the cold-scale model (L*=1/13=0.077 and, thereby, u_{mf}=0.0043 m/s) could be attained with a particle diameter of 35 μm, which assigns it to the Geldart group B solids. With this, a cold-scale model resembling the reference boiler with a scale factor of 1/13 was designed and built according to Glicksman's simplified set of scaling laws, with the scaling parameters listed in Table 2. For the constructed scale model, the corresponding up-scaled values are given in parentheses, indicating the error incurred when the exact values derived from the scaling laws cannot be applied in practice. For example, the copper solids employed are lighter than the specification and scale up to a value of 2,468 kg/m^3 rather than the density of the material in the reference boiler (2,600 kg/m^3).

The constructed scale model is also operated with solids (glass beads, d=112 μm and ρ=2,600 kg/m^3) that do not respect the simplified scaling proposed by Glicksman. However, if the further-simplified scaling laws derived by van der Meer and colleagues [56] are used, these runs could be scaled up to large-scale, hot conditions (see the last column in Table 2). The up-scaled hot unit would then correspond to one with a cross-sectional area of 2.1 m^2 and a height of 6.5 m. Note, however, that the further simplification of these scaling laws restricts the scaling validity to the viscose regime (i.e., up-scaled gas velocities not higher than 2.7 m/s) [56]. While the cold unit still yields aspect ratios for the dense bed and the furnace that are characteristic for CFB boilers, the freeboard may be too short to ensure that all the runs have a fully developed transport zone similar to that present in CFB boilers.

2.2.2 Validation of the fluid-dynamical down-scaling

Validation of the cold-flow model is performed on the basis of four reference cases, with loads ranging from 60% to 100% and solids concentrations at the top of the furnace ranging from 0.4 to 3.0 kg/m^3. The comparison of particle concentration profiles shows very good agreement for all four reference cases, which means that the scaling is considered to be successfully validated.

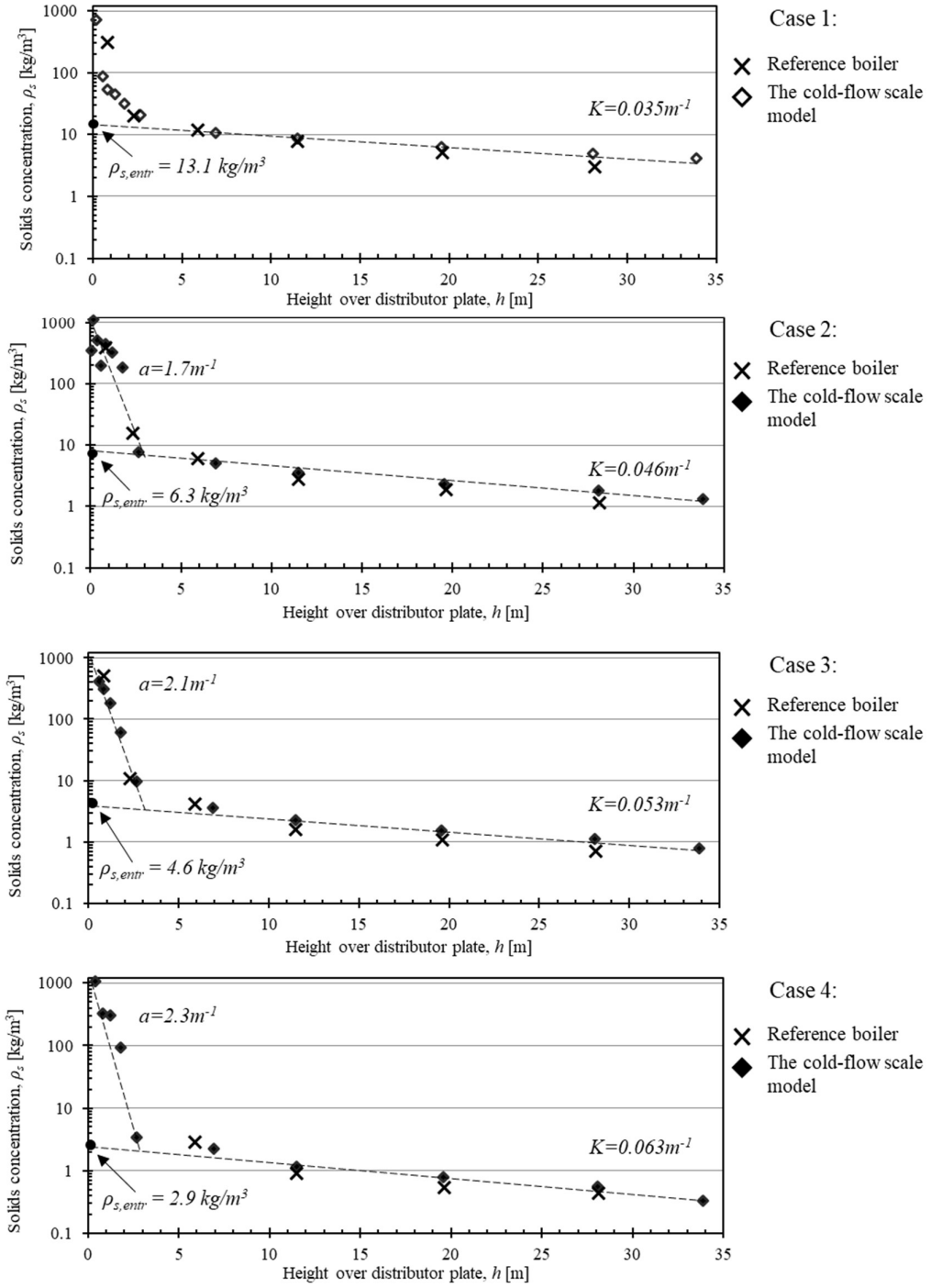

Figure 2. Comparison of solids concentration profiles between the reference 200-MW_{th} CFB boiler and the corresponding cold-flow scale model. Source: Paper III.

3. Experimental work

3.1 Experimental setup

In the present work, two experimental units were used: a pseudo-2-dimensional (pseudo-2D) unit (**Paper I**); and the above-mentioned cold-flow scale model (**Papers II** and **III**) of a 200-MW_{th} CFB boiler. Table 3 shows the main dimensions and operational parameters for the three experimental setups described in each of the papers.

Table 3. Experimental setups used in this work. Up-scaled values are given in parentheses.

			Paper I	**Paper II**	**Paper III**
			Pseudo-2D unit	*Cold-flow scale model* (non-scaled material)	*Cold-flow scale model* (scaled material)
Cross-sectional area	D x W	m^2	0.7x0.12	0.45	0.45 *(75)*
Height	L	m	8.5	3.1	3.1 *(40)*
Particle diameter	d_p	μm	316	112	35 *(195)*
Particle density	ρ_p	kg/m^3	2600	2600	8920 *(2480)*
Minimum fluidization velocity	u_{mf}	m/s	0.067	0.013	0.0045 *(0.0162)*
Terminal velocity	u_t	m/s	2.21	0.64	0.28 *(1.01)*
Fluidization velocity	u_0	m/s	[0.3-7.0]	[0-1.4]	[0.17-1.25] *([0.6-4.5])*
Pressure drop across riser	ΔP_{Riser}	kPa	[1.7-10.5]	[0.15-1.5]	[0.9-2.3] *([3.2-8.4])*
Fluidization velocity in G_s valve	$u_{Gs,valve}$	m/s	-	$1.5u_{mf}$	$4.5u_{mf}$

The overall experimental setup is similar for all the cases: the fluidizing air is fed by two inlet fans coupled in series and controlled with flowmeters and valves through a LabView interface. Pressurized air is used for auxiliary systems, such as those controlling fluidization of the particle seal and purging of the pressure sampling lines. The air distributor plates provide a pressure drop that is sufficiently low to ensure the same bottom bed regime as is used in industrial units. A cyclone separates the externally circulating particles from the air flow, and a particle seal ensures recirculation of the solids into the riser without bypass of gas up through the cyclone. The concentration of solids in the riser is measured by differentiation of the pressure measurements, and the rate of solids circulation is estimated using a butterfly valve with an in-built air plenum that is placed in the cyclone leg. The different solids used in the papers are all members of the Geldart B group.

3.1.1 Pseudo-2-dimensional unit

Figure 3 shows the bottom part of the pseudo-2D unit with the dimensions of the riser being 0.7×0.12×8.5 m^3 (for further details, see Table 3). The depth of 0.12 m in combination with the bed material used (glass beads) means that there is no formation of solids wall layers along the long front and back walls, so the solids flow is visually accessible thanks to the transparent front wall frames. The width of 0.7 m entails the formation of solids wall layers along the short right and left walls, so the solids flow is visible along its thickness from the front wall. In summary, the unit enables visual access to the qualitative solids flow established in a vertical slice of a CFB boiler. The unit also has sufficient height to allow a fully developed transport zone. The 24 pressure measurements are densely spaced in the bottom of the riser, with 11 taps located within the first meter above the grid.

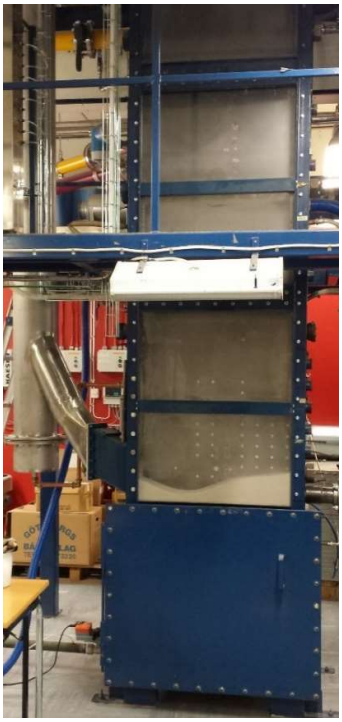

Figure 3. Photograph of the bottom part of the pseudo-2D unit.

3.1.2 Fluid-dynamically down-scaled unit

The cold-flow scale model and associated instrumentation used in this work are depicted in Figure 4 and in a 3D depiction of the cold-flow scale model in Figure 5. For this setup, a suction fan and a filter were installed downstream to ensure that the bed pressure was maintained below the atmospheric pressure (thus avoiding potential leakage of the bed material) and to allow control of the atmospheric-pressure height in the riser, similarly to commercial CFB boilers.

The riser of the unit is equipped with 15 pressure transducers. This is in stark contrast to the pressure data collection systems used in commercial boilers, in which only a few (typically, 3–

5) transducers are placed in the riser, yielding a much lower spatial resolution of the solids concentration profile.

Two different bottom configurations were used: tapered walls were used to resemble the riser geometry of the reference boiler in the scaling validation cases described in **Paper III**, while vertical bottom walls were used for further measurements. The unit has lateral air injection points at three different heights, which are used for the injection of recirculated flue gas and secondary and tertiary air. The cyclone is not scaled but is modeled to ensure that the bed material is retained within the circulation loop. This requires a slightly modified shape of the loop seal, which is designed to contain the resembled volume of solids in the reference boiler.

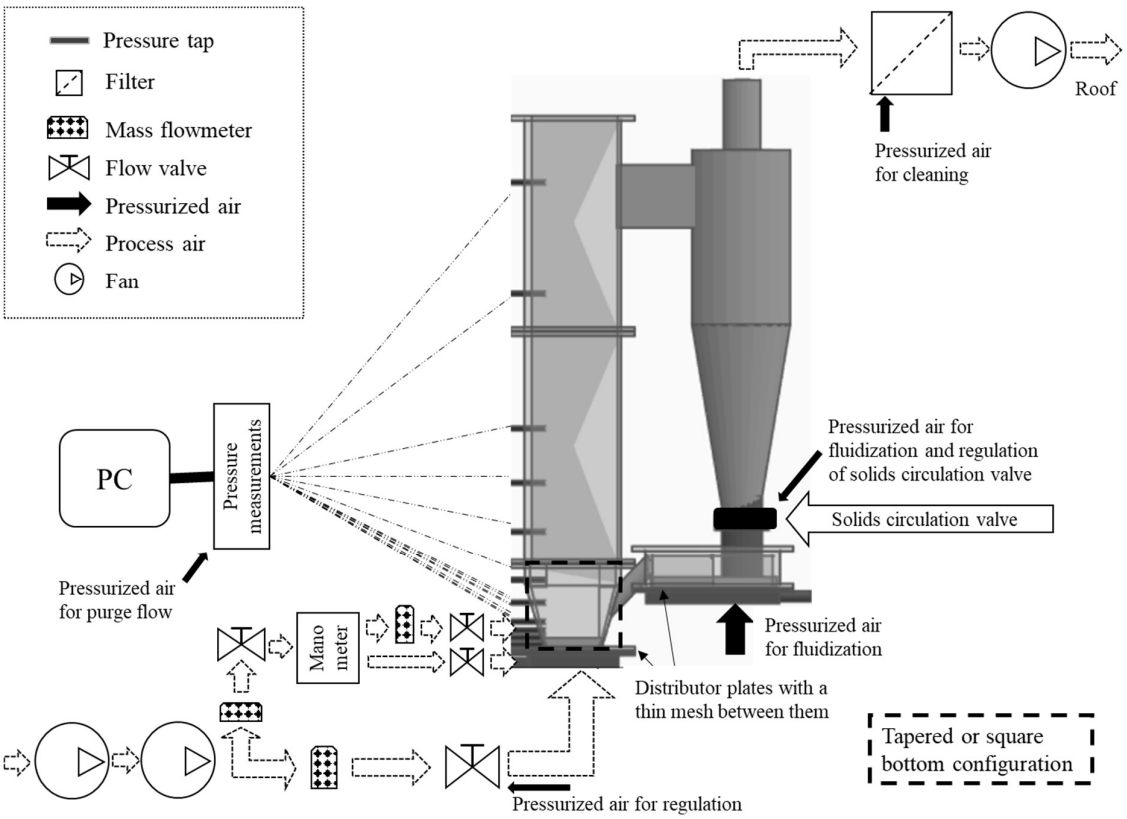

Figure 4. Schematic of the cold-flow scale model and its instrumentation. Source: Paper III.

The cold-flow scale model unit was used for the experiments in **Papers II** and **III**, as described in Table 3. The unit is down-scaled with Glicksman's simplified scaling laws (see Section 2.2.1). Silica glass particles not fulfilling the Glicksman's scaling laws were used for **Paper II** (Figure 6a) and copper particles fulfilling Glicksman's scaling laws were used in **Paper III** (Figure 6b).

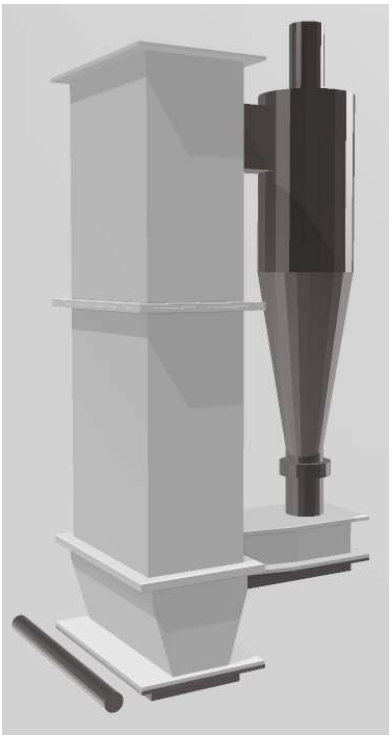

Figure 5. 3D depiction of the cold-flow scale model.

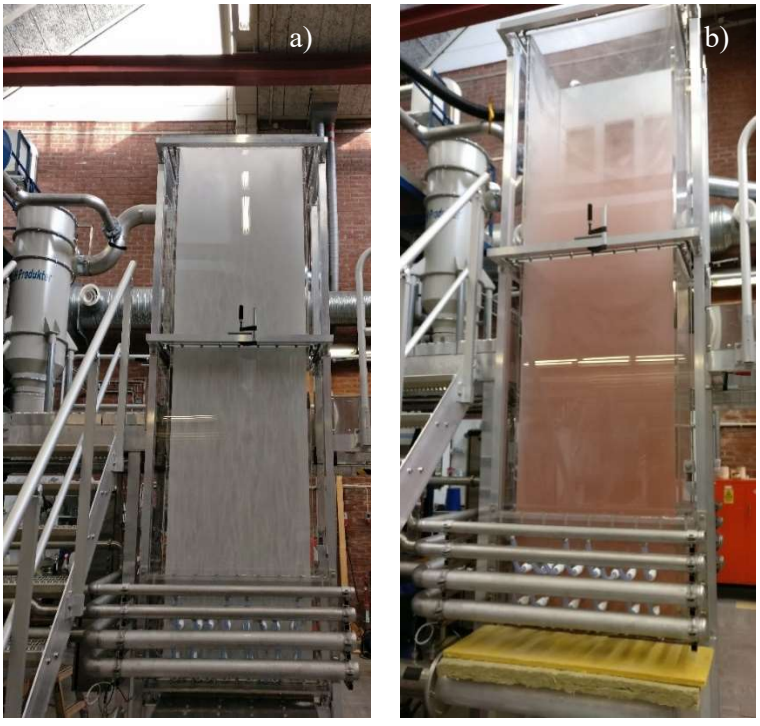

Figure 6. Photographs of the: a) cold-flow scale model with non-scaled particles (glass particles); and b) cold-flow scale model with scaled particles (copper).

3.2 Experimental procedures

The high number of pressure transducers along the riser allows for the determination at a relatively high spatial resolution of the vertical profile of the particle concentration. The distance between pressure transducers varies along the riser, being shortest in the bottom region (in the order of 0.5–1.0 cm) and longest at the top (up to 50–100 cm, depending on the unit). Thus, this work provides data with uniquely high resolution for the bottom region. From the measurements made in the bottom region, the following three categories are established in terms of the presence or absence of a dense bed (summarized in Table 4):

- **Presence of a dense bed**. The pressure measurements show a linear decrease with height of the riser. To assess this, a minimum of three pressure measurements within the dense bed is needed [33]. Note that a typical dense bed height for CFB boilers is reported in literature as 0.4–0.6 m, and it decreases with the fluidization velocity [33].
- **Uncertain presence of a dense bed**. Although a linear pressure decrease is not observed, a dense bed that is lower than the height of the third pressure tap could still be present, since a solids concentration >750 kg/m^3 (which shows that the emulsion phase occupies a larger volume than the bubble phase) is noted.
- **Absence of a dense bed**. Neither a linear pressure drop nor a dominant emulsion phase is observed.

The symbols listed in Table 4 are used in all the papers to indicate to which of the above-mentioned categories the bottom region belongs.

Table 4. Criteria used to categorize the experimental runs in terms of the fluid dynamics in the bottom region. Source: Paper III.

Category	Dense bed present?	*Symbol*		*Criterion 1:* Linear pressure drop across three bottom measurements	*Criterion 2:* bubble fraction <0.5
1.	yes	■	Filled	yes	yes
2.	unclear	◓	Half-filled	no	yes
3.	no	□	Not filled	no	no

The external solids circulation is measured with a butterfly valve, which once it is closed fluidizes the material accumulating above it in the downcomer. The rate of circulation of solids is calculated from the rate of the pressure increase, as illustrated in Figure 7.

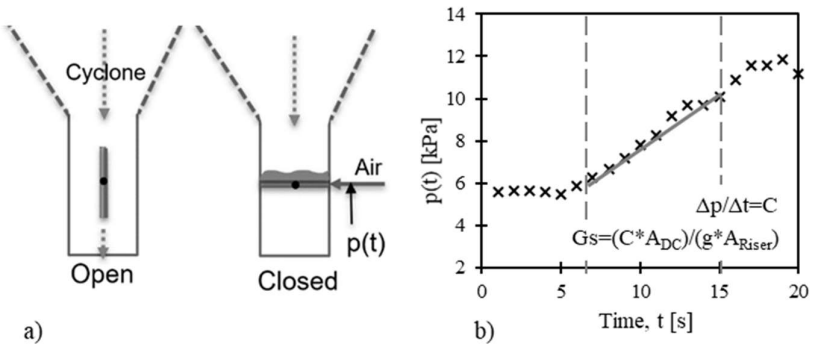

Figure 7. Measurement of the external solids circulation. a) Schematic showing the functionality of the butterfly valve in the downcomer. b) Transient pressure increase and corresponding solids circulation. Source: Paper III.

Particle size segregation was studied in the scaled unit, with particles being sampled at the bottom bed and at the particle seal after abrupt defluidization of the unit. The particle samples were analyzed using laser diffraction.

4. Results and Discussion

The results obtained from this work include: 1) qualitative data (**Paper I**, pseudo-2D unit); 2) quantitative data, with limited relevance to large-scale CFB boilers (**Paper II**, where the 3-D unit avoids the dominance of wall effects and according to the most simplified scaling laws resembles a small CFB boiler; see Table 2); and 3) data that represent a 200-MW_{th} CFB boiler over its entire operational range (**Paper III**).

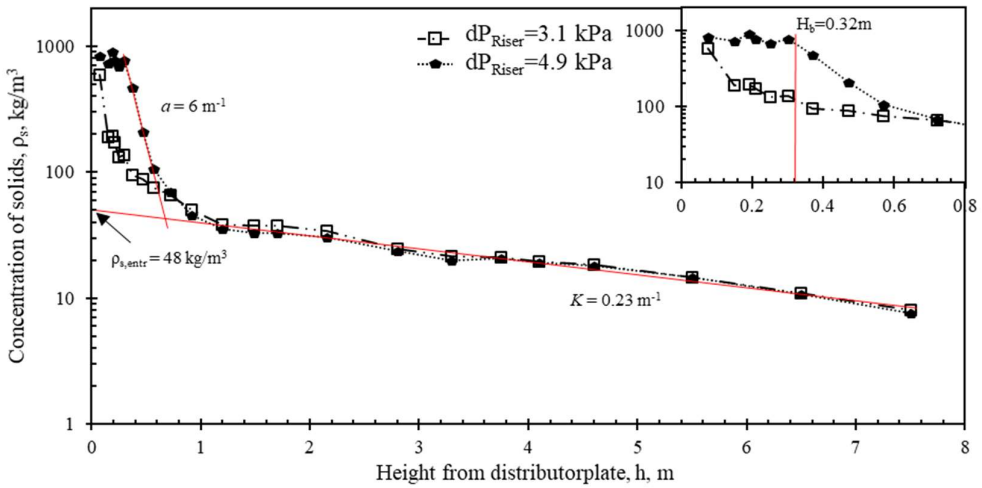

Figure 8. Solids concentration profiles in the pseudo-2D unit, at constant fluidization velocity (4 m/s) and with varied solids inventory (riser pressure).

Typical solids concentration profiles are depicted in Figure 8 based on measurements carried out in the pseudo-2D unit, with and without a dense bed, where the used parameter for the case with a dense bed is marked. A graphical overview of the solids flow pattern with the main findings of this work is given in Figure 9 and the results show that: A) a dense bed (revealed by a bottom region with a height-independent solids concentration) is only present for runs with sufficient solids loads (riser pressures) for each gas velocity; B) a splash zone is formed directly above the dense bed (or the distribution plate if no dense bed exists) with a steep decrease in solids concentration with decay coefficient a varying depending on the presence of a dense bed and its height; C) the solids entrainment from the bottom region, $\rho_{s,entr}$, is observed to depend on the presence/absence of a dense bed, but not on its height; D) the solids back-mixing to the wall layers in the transport zone, described by the decay coefficient K, is observed not to be affected by the characteristics of the bottom region; E) the measured external circulation of solids flux compared to the upwards solids flux shows the weakness of the assumption of the external circulation of solids being equal to upwards solids flux; and F) the backflow ratio of solids in the top describes the increase in back-mixing with changes in fluidization velocity. The following subsections give more-detailed descriptions of these key results.

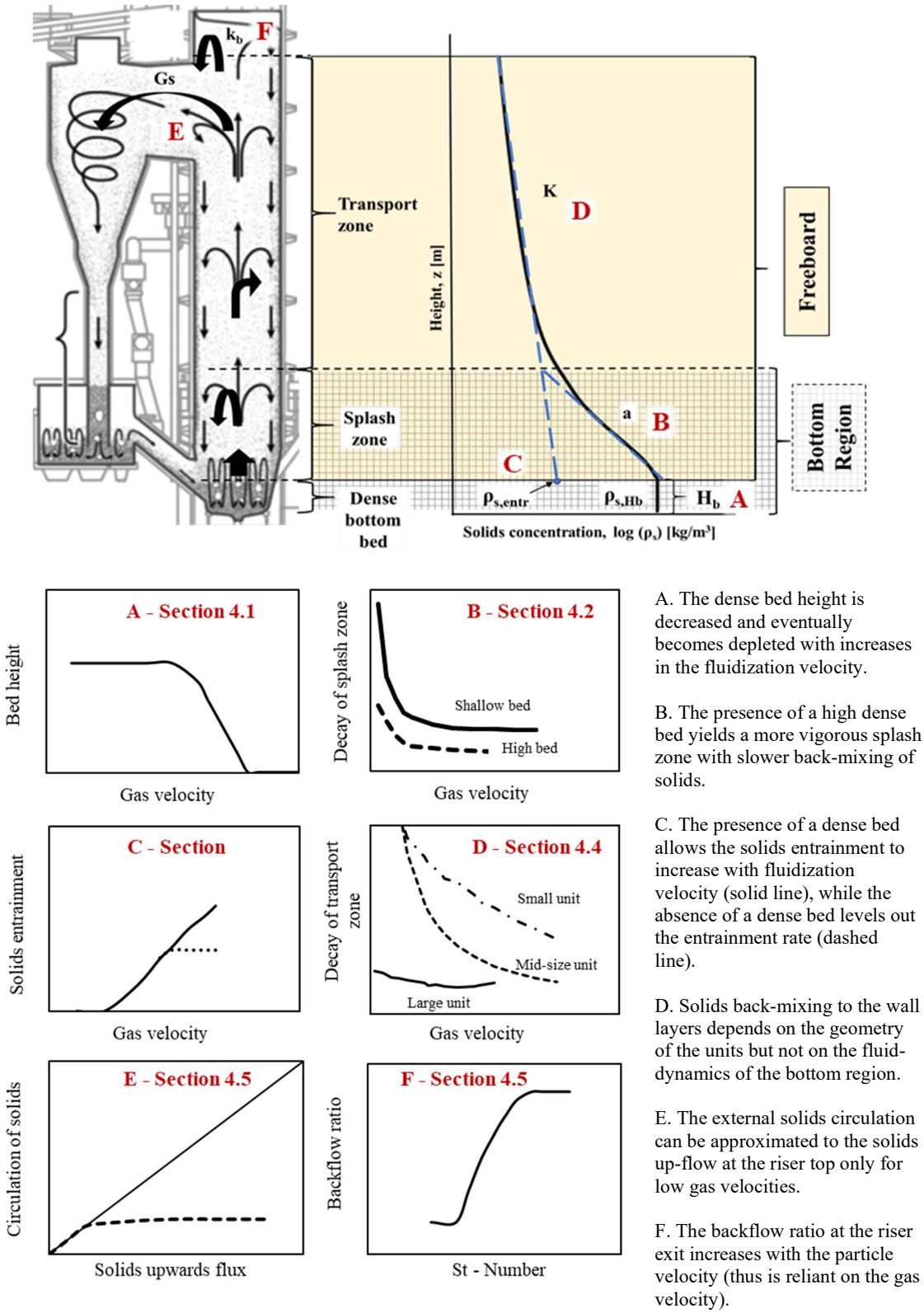

A. The dense bed height is decreased and eventually becomes depleted with increases in the fluidization velocity.

B. The presence of a high dense bed yields a more vigorous splash zone with slower back-mixing of solids.

C. The presence of a dense bed allows the solids entrainment to increase with fluidization velocity (solid line), while the absence of a dense bed levels out the entrainment rate (dashed line).

D. Solids back-mixing to the wall layers depends on the geometry of the units but not on the fluid-dynamics of the bottom region.

E. The external solids circulation can be approximated to the solids up-flow at the riser top only for low gas velocities.

F. The backflow ratio at the riser exit increases with the particle velocity (thus is reliant on the gas velocity).

Figure 9. Graphical abstract of the main results from the three papers. The lines in the figures are for displaying the concept.

4.1 Bottom bed

The presence of a dense bed has been demonstrated in specific CFB units, and the height of the bed decreases with increasing fluidization velocity [33]. In this thesis, at least one of the experimental cases described in each paper shows that the dense bed is lost as the fluidization velocity is increased, with progressive depletion of the dense bed as more material is lifted to higher locations in the riser [61]. Figure 10 shows how the dense bed height decreases with fluidization velocity in three different units: the pseudo-2D unit (**Paper I**); the scale model (**Paper III**); and the 12-MW_{th} Chalmers CFB boiler [33]. Thus, the presence of a dense bed in CFB boilers is expected but requires a sufficient level of bed material in the riser. An increase of mass in the system is required to maintain a dense bed height, with increasing fluidization velocity [43]. Monitoring the presence of a dense bed requires the use of densely spaced pressure taps in the bottom region, which is not the case in commercial CFB boilers. Thus, it is likely that some commercial CFB boilers operate without a dense bed, although some monitoring of the pressure drop in the lower region (extending over some meters) of the furnace is typically implemented. The lowest detectable dense bed height depends on how densely spaced the pressure taps are (a minimum of three pressure points is required). While a dense bed can exist below this height, the concentration between the lowest measuring points must be assessed to reveal its possible presence.

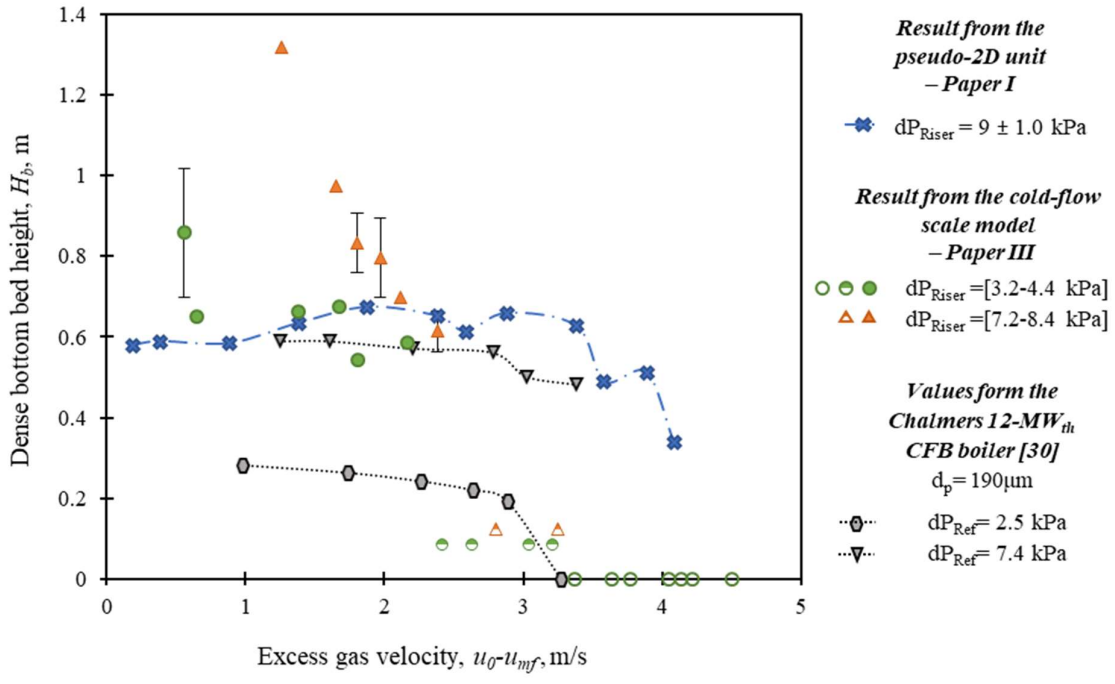

Figure 10. Dense bottom bed height as a function of excess gas velocity. The dense bed is eventually depleted if the riser pressure drop is kept constant and at a low value, with increasing fluidization velocity. The figure is based on data from Paper I, Paper III, and published values acquired from the 12-MW_{th} Chalmers boiler [33]

Even if the dense bed height is relatively stable for an initial increase in the fluidization velocity, it rapidly declines as the fluidization velocity increases while at the same time the local solids concentration decreases (see the measurement data from the pseudo-2D unit in Figure 11). Eventually, the yielded values correspond to a situation in which the volume occupied by bubbles equals that occupied by the emulsion phase (dashed line in Figure 11). Few reports have been published on the bottom bed in CFB units and even fewer studies have investigated the fluid-dynamical conditions that exist after the dense bed is depleted [33].

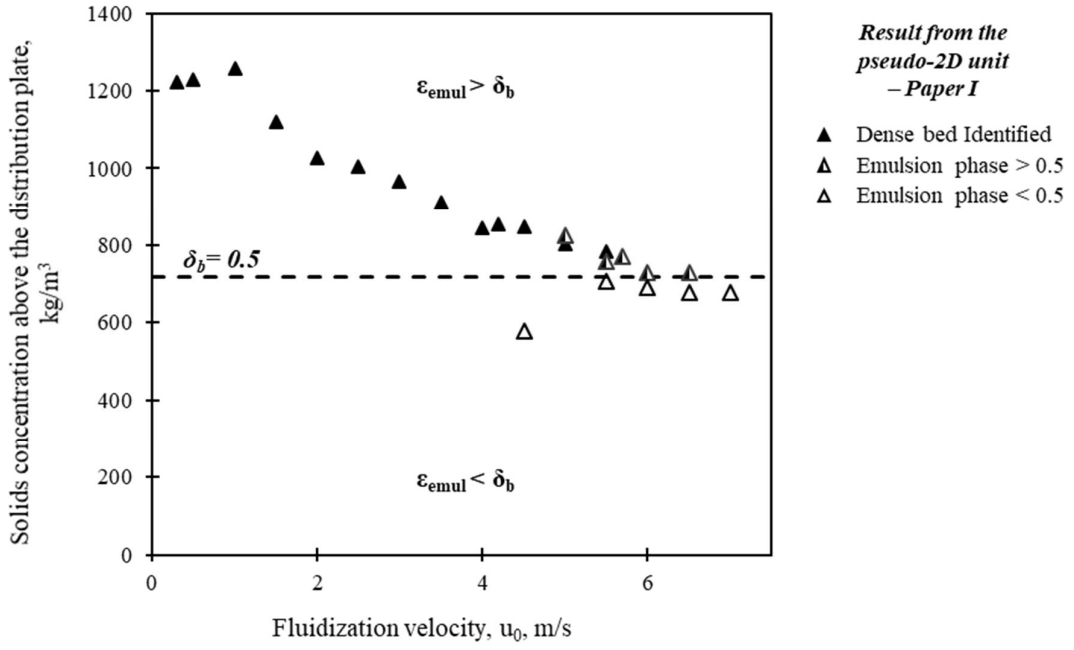

Figure 11. Solids concentration above the distribution plate as function of fluidization velocity. No dense bed is detected for those cases in which the emulsion phase occupies less volume than the bubble phase. Source: Paper I.

4.2 Splash zone

The presence of a splash zone has typically been explained in terms of the ejection of particle clusters through bubble bursting at the dense bed surface and their back-mixing to the dense bed in a ballistic fashion. This mechanism implies that the bubble size and velocity (strongly dependent upon the dense bed height and fluidization velocity) should play key roles in the vertical extent of the splash zone. While the dependence of the splash zone back-mixing on fluidization velocity has been known from earlier studies [14, 34], the present work reveals the dependence on the height of the dense bed. This is shown in Figure 12, where greater riser pressure drops (i.e., taller dense beds) yield a lower decay constant at a given fluidization velocity.

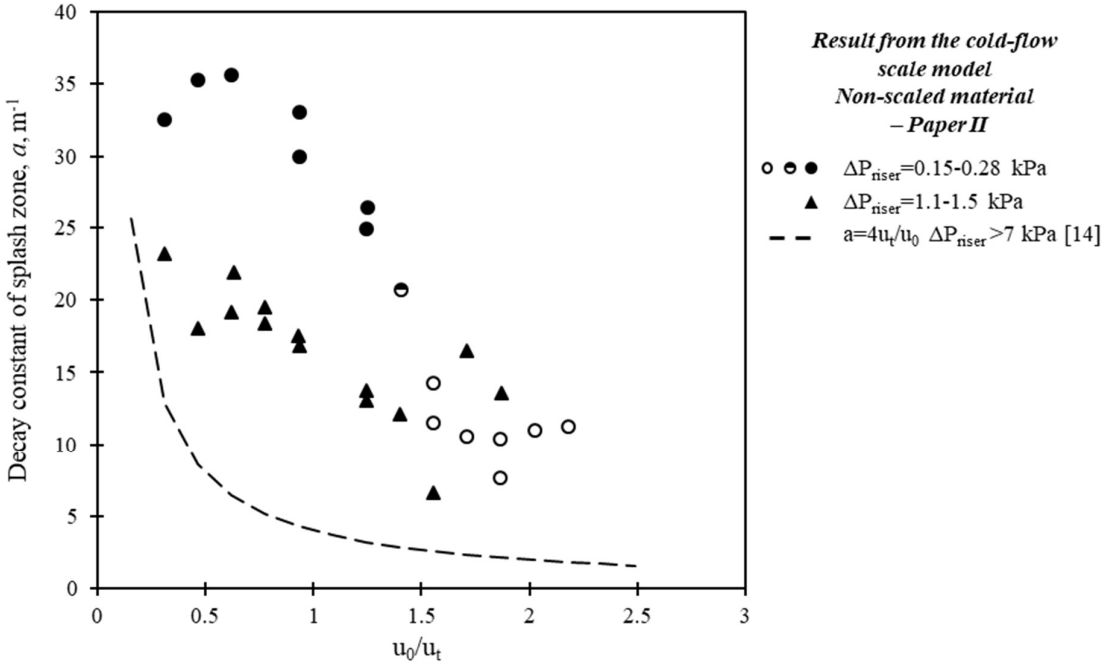

Figure 12. The decay coefficient of the splash zone in the scale model operated with non-scaled material. Source: Paper II.

Note that this work also reveals (as shown in Figure 8 and described in Section 2.1) the existence of a splash zone in cases without a dense bed. This requires revision of the traditional understanding of the splash zone as back-mixing induced by bubbles in the dense bed reaching the dense bed surface and bursting. A more general hypothesis that has been put forward is that the particle clusters forming the splash zone are ejected by local and regular occurrences of high-velocity gas, which originate from either bubble bursts at the dense bed surface (in the presence of a dense bed) or bed-plenum interactions in the fluidization nozzles (in the absence of a dense bed) [61].

4.3 Solids entrainment

Data from all three papers in this work show that solids entrainment increases with fluidization velocity as long as a dense bed is maintained (with the height of the dense bed not affecting the rate of entrainment) and levels out when the dense bed is depleted. This is exemplified by the experimental data from the cold-flow model shown in Figure 13a.

Figure 13b compares data on solids entrainment from different sources: the cold-flow model used in this work (operated with [**Paper III**] and without [**Paper II**] scaled bed material); and the Chalmers 12-MW_{th} CFB boiler [14]. Only those cases with confirmed presence of a dense bed are included for the sake of comparison (as depletion of the dense bed strongly affects the solids entrainment, see discussion above). It is here observed that the solids entrainment is independent of the cross-sectional geometry and size of the boiler.

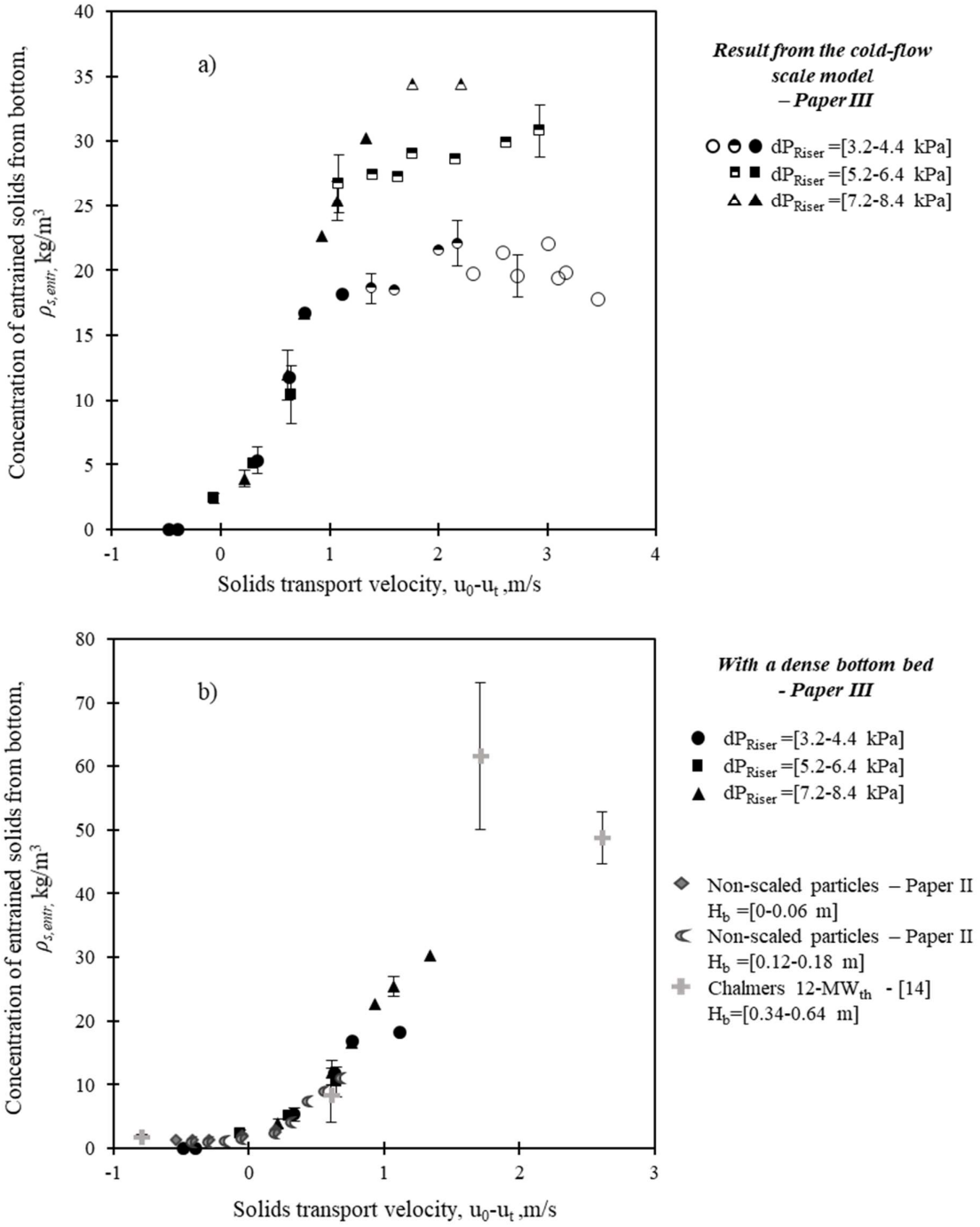

Figure 13. Solids entrainment as a function of the excess transport velocity: a) sampled through the scale model of a 200-MW_{th} boiler, from Paper III where secondary air is excluded: and b) comparison of the data in the presence of a dense bed from different publications and units. Source: Paper III.

4.4 Transport zone

The back-mixing of entrained solids to the wall layers, described by the decay coefficient *K*, is found to be dependent upon the fluidization velocity (Figure 14), in line with previous findings in the literature [14] (the correlation derived from data from the Chalmers boiler is also plotted). Figure 14 shows that this coefficient remains unaffected by the presence or absence of a dense bed in the bottom region. Instead, a strong dependency on the size of the unit is observed: the strongest back-mixing (highest decay constant) is found in the smallest unit (pseudo-2D) and the weakest back-mixing is seen in the modeled 200-MW_{th} CFB boiler, while the back-mixing levels from the Chalmers 12-MW_{th} boiler lie between these two values.

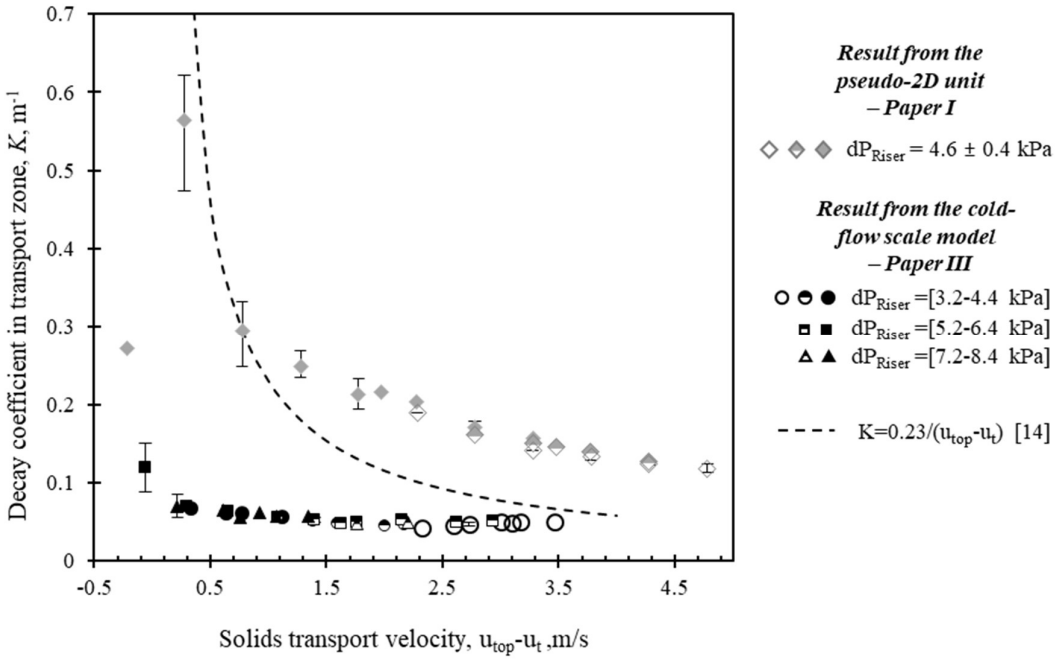

Figure 14. Decay coefficients for the solids concentration in the transport zone for three units of different size scales. Based on results from Paper I , Paper III and with correlation from [14].

The solids back-mixing in the transport zone occurs through the net transfer of solids from the core to the wall layers. Assuming a horizontally well-mixed core region, Johnsson and Leckner derived the dependency between the decay coefficient, *K*, and the mass transfer coefficient, *k*, as follows [14]:

$$K = \frac{4k}{D_e(u-u_t)} \tag{10}$$

where D_e is the hydraulic diameter, which the mass transfer for rectangular geometries translates into:

$$k = K(u-u_t)\frac{L_x L_y}{2L_x+2L_y} \tag{11}$$

The values for the mass transfer coefficient governing the back-mixing in the transport zone are plotted in Figure 15, which includes data from the scale model (**Paper III**) and values from large CFB boilers in litterture, the 12-MW_{th} Chalmers CFB boiler, and the pseudo-2D unit [14, 17, 18, 20-22]. The larger geometries show consistently higher values, revealing a relationship between the size of unit and the magnitude of mass transport from the core to the wall layer.

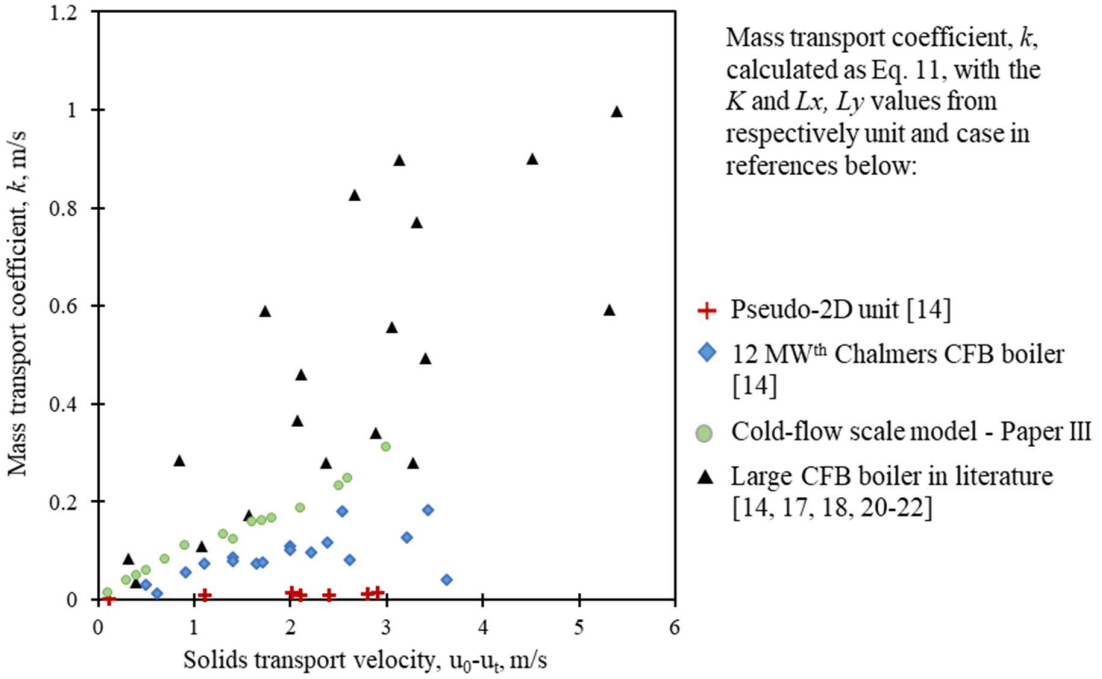

Figure 15. Mass transfer coefficients for solids back-mixing to the wall layers, *k* [m/s]. Values are taken from units with different size scales [14, 17, 18, 20-22].

4.5 Exit backflow

The solids flux at the top of the riser increases with fluidization velocity, as exemplified in Figure 16 by data collected from the scale model. The figure also shows the flow of solids that are circulating externally, measured according to the method summarized in Section 3.2. A remarkable difference is observed between the solids up-flow at the top of the riser and the external solids circulation, at higher fluidization velocities, which indicates a significant back-flow effect at the riser exit.

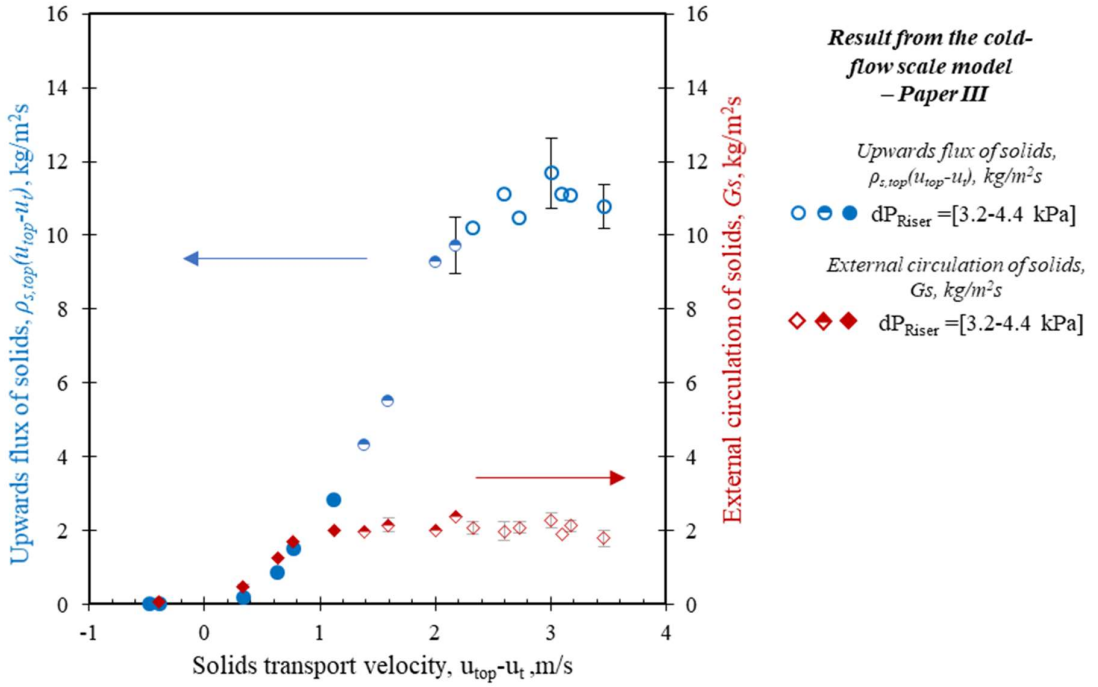

Figure 16: Solids up-flux at the riser top (estimated from the local solids concentration) compared to the external solids flux (measured with a fluidizing butterfly valve). Based on results from Paper III.

In the literature, it has been common to estimate the solids external circulation by assuming that it is roughly equal to the up-flow at the riser top (the calculation of which from pressure measurements is straightforward). Note that, due to solids size segregation along the riser, the assumption that the terminal velocity used to approximate the solids up-flow is problematic. At low fluidization velocities, the size segregation is high and if one assumes well-mixed solids this typically yields a significant overestimation of the terminal velocity at the riser top (resulting in an underestimation of the up-flow). This work applied solids sampling in **Paper III,** in bottom of riser and loop-seal to monitor the solids size segregation. The results presented in Figure 16 and **Paper III** show that solids circulation values from the literature estimated from measurements in the riser may be consistently higher than the real values, revealing a significant backflow effect at the riser exit. At low gas velocities (i.e., low values of the solids upwards flux), all solids reaching the riser top are externally circulated, i.e., the backflow is negligible (k_b~0), as seen in Figure 16. However, the backflow becomes significant at higher gas velocities.

The Stokes (*St*)-number, describing the extent to which the inertia of a particle makes it unable to be dragged by a fluid, is in Figure 17 chosen to describe the phenomenon of backflow, as the solids backflow originates from the inability of solids to follow the gas stream as it curves into the exit duct to the cyclone. As shown, the backflow is almost non-existent at low Stokes numbers, and there is a transition along *St*-numbers in the range of 0.08–0.12 such that the backflow increases rapidly before eventually levelling out at *St*-numbers above 0.12. Theoretically, the backflow ratio should continue to increase until unity for even higher gas

velocities, with all the particles being internally recycled and disengaging fully from the gas stream.

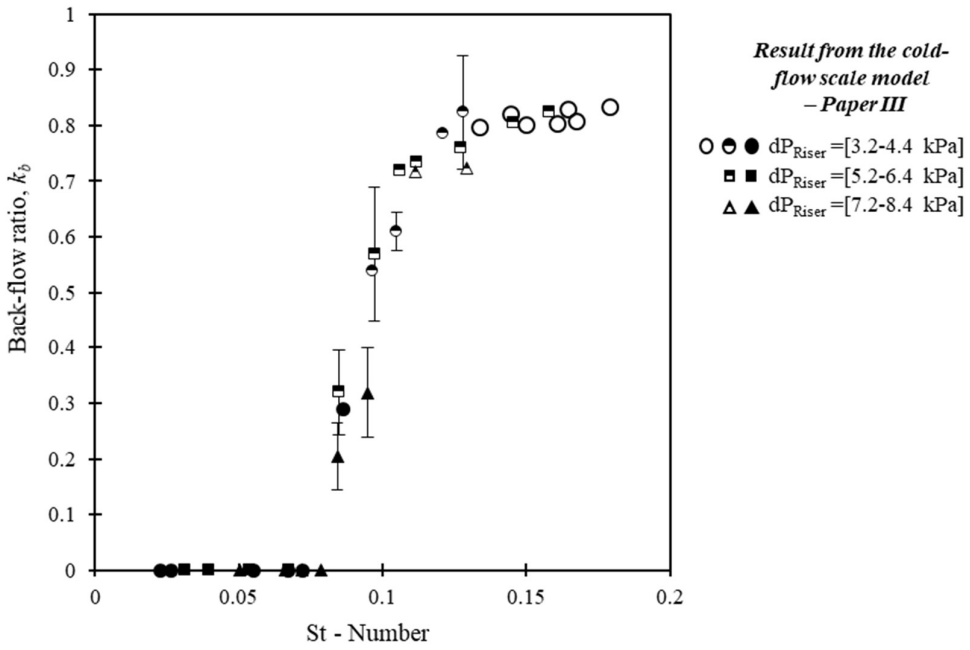

Figure 17 Solids backflow ratio as a function of the Stokes (*St*)-number. Data are from the cold-flow scale model representing a 200-MW_{th} CFB boiler. Source: Paper III.

5. Conclusions

The solids flow patterns in CFB units studied in different units and under various conditions show the same governing mixing mechanisms when the scope specification (Geldart B group, low aspect ratios of the furnace and the bottom bed, moderate circulating solids fluxes) is respected.

A cold-flow model that fluid-dynamically resembles an existing 200-MW_{th} CFB boiler, built and operated according to the Glicksman's simplified set of scaling laws, is shown to reproduce accurately the fluid dynamics of the reference large-scale boiler. The experiments of this thesis work provide a set of qualitative and quantitative data-points relevant to large CFB boilers.

The solids external circulation is shown to be the result of a series of underlying sequential events. Some of these phenomena, such as the presence/absence of a dense bed, have strong effects on the mixing processes further downstream in the riser. The presence of a dense bed or of a taller dense bed yields a more vigorous splash zone with slower back-mixing of the solids. The presence of a dense bed also allows the solids entrainment to increase with fluidization velocity, while the absence of a dense bed levels out the entrainment rate. The extent of solids back-mixing to the wall layers depends on the geometry of the unit but not on the fluid dynamics of the bottom region. The backflow ratio at the riser exit increases with the particle velocity (and, thus, the gas velocity). The backflow cannot generally be considered to be negligible, as the external circulation of solids is typically significantly different from the solids up-flow at the riser top.

6. Future Work

Listed below are avenues of research – together with key questions - linked to the present work that could provide further insights into the solids flow patterns in CFB boilers.

- *Solids back-mixing to the wall layers*: What is the underlying mechanism governing back-mixing in the transport zone and mass transfer from core to wall layers, and which dependencies are established?

- *Solids back-mixing in the splash zone*: Can this back-mixing be mechanistically described by means of a model, which includes its dependency on the dense bed height?

- *Back-flow effect*: Can this local solids back-mixing be generally described for different boiler sizes through a Stokes number that includes a characteristic length?

- *Solids entrainment*: How is it affected by the presence of tapered walls?

- *Bottom region*: In the absence of a dense bed, what solids flow pattern is established and what causes the appearance of a splash zone?

Furthermore, fluid-dynamical studies beyond those related to the solids flow would be of interest in such a scale model of a large-scale boiler. For example, it would be valuable to implement a particle tracking system for the study of fuel mixing.

7. Acknowledgments

This thesis and the work on which it is based would not have been possible without help from many people. I will always be thankful for all the help, support and encouragement that I have received over the years.

First, I would like to thank my two supervisors, Associate Professor David Pallarès and Professor Filip Johnsson, for giving me this opportunity in the first place and for guiding me through the jungle of experimental work in a CFB unit. Filip – thank you for all the questions and backup, resulting in a better and deeper discussion and result. David – this thesis and its content would not have been possible at all if you had not been there, always offering another solution, always reading, commenting and fixing things.

Ulf Stenman and Rustan Hvitt are my Superheroes. Ulf – thank you for helping me overcome all the experimental obstacles in The Big Blue and the building of S-13, always trying to solve the issues and teaching me how LabVIEW works. Rustan – thank you for your assistance with the big build of S-13, spending days reconfiguring the S-13, and wondering why it doesn't work when Murphy is sitting on top of everything.

I am grateful for the financial support from the Swedish Energy Agency (project no. 38347-2) and Valmet Technologies Oy, with special thanks to Ville Ylä-Outinen. Several persons have helped me with the construction of the S-13, including the Research Engineers at Chalmers, Elwe Aluminium och Rostfritt, Interpipe, MK Engineering, MA-composit, and VVS-teknik Göteborg. I also gratefully acknowledge Andreas Holzer, Matti Grabo and Alīna Bancevič̆a for providing the CAD drawings. Professor Bo Leckner – thank you for always having time to answer my questions on CFB units.

I am grateful for the strong support that I received from the Department, particularly when the days were heavy and life was upside-down. My managers allowed me to work on my own terms, friends and colleagues were supportive and inspiring, and there was always someone around who had an answer or a new question. To my roommates, Guillermo and Huong – thank you for keeping me sane. Thanks also to Rikard, Anna, Jesper and Angelica for always being positive and supportive. Erik: thank you for always showing interest in my work. Adrian – over the 10 years that we have spent together at Chalmers, you have been boosting me daily, helping me to perform better and to continue with the day-to-day tasks. I also received strong support from friends outside Chalmers: Lotta, Karin and the rest, the Chalmers friends, the Archery friends, the Flabäck friends, the stable girls, and all the other people who are part of my life.

Last but not least, my biggest supporters are the members of my family, we fight till the end. Dad - you are always missed and always remembered. Mum – thanks for showing me that this is possible and supporting me at every step. Pontus – always with a smile, trying to make everyone happy. Lotti and Håkan – thanks for giving me some peace of mind. My love, Sebastian, there are no words for what you give me. I can only be grateful that you are sitting beside me in the roller-coaster that is our life. Theodor, our little joy and hurricane, Mommy loves you!

Yours truly!

Tove

8. Nomenclature

a	Decay coefficient of the splash zone	[1/m]
A_{**}	Cross-sectional area	[m^2]
D	Equivalent riser diameter	[m]
d_p	Particle diameter	[µm]
g	Gravity constant, 9.81 m/s^2	[m/s^2]
G_s	External circulation of solids	[kg/m^2s]
$G_{s,**}$	Solids flux	[kg/m^2s]
h	Height over distributor plate	[m]
H_b	Dense bed height	[m]
H_{Top}	Top height of the riser	[m]
k	Net mass transfer coefficient	[m/s]
K	Decay coefficient of the transport zone	[1/m]
k_b	Back-flow ratio	[-]
L	Length	[m]
L^*	Scale factor for length	[-]
Lx, Ly	Dimensions of the risers	[m]
m^*	Scale factor for mass	[-]
PSD	Particle size distribution	[-]
St	Stokes number	[-]
t^*	Scale factor for time	[-]
u^{**}	Fluidization velocity	[m/s]
u_0	Fluidization velocity	[m/s]
u_{mf}	Minimum fluidization velocity	[m/s]
u_t	Terminal velocity	[m/s]
z	Height in the riser	[m]
δ_b	Bubble fraction	[-]
ΔP_{**}	Pressure drop	[Pa]
ε_{emul}	Fraction of emulsion	[-]
μ_g	Viscosity	[Pas]
ρ_{**}	Density, Concentration	[kg/m^3]
$\rho_{s,**}$	Solids concentration in **	[kg/m^3]
$\rho_{s,entr}$	Concentration of entrained solids from bottom region	[kg/m^3]
Φ	Particle sphericity	[-]

Subscripts **

b	Dense bed
cluster	Bubble eruption into the splash zone
core	Values from the core

DC	Down-comer
disperse	Dispersed phase into the transport zone
g	Gas
Gs,valve	Values at the solids circulation valve
Hb	Values at the dense bed
layer	Values in the wall layer
p	Particle
Ref	Reference values measured in the range of h=0.1–1.6 m
Riser	Riser, values measured for h=0.1 m - top of the riser
s	Solids
seal	Value in particle seal
top	Value at the top of the riser

9. Bibliography

1. IEA, *Energy, Climate Change and Environment 2016 Insights*, I.E. Agency, Editor. 2016: Paris, France.

2. Leckner, B., L. Thorson, J. Kjärstad, and F. Johnsson, *Utilization of fluidized bed boilers ---a worldwide overview*, in *Developments in Fluidized Bed Conversion 2011 to 2016*. 2016, IEA-FBC TCP: Presented at IEA-FBC 73rd Technical Meeting, Tokyo, Japan (December 2016).

3. Koornneef, J., M. Junginger, and A. Faaij, *Development of fluidized bed combustion—An overview of trends, performance and cost.* Progress in Energy and Combustion Science, 2007. **33**(1): p. 19-55.

4. Obernberger, I., *Decentralized biomass combustion: state of the art and future development.* Biomass Bioenergy, 1998. **14**(1): p. 33-56.

5. Leckner, B., *Fluidized bed combustion: mixing and pollutant limitation.* Progress in Energy Combustion Science, 1998. **24**(1): p. 31-61.

6. Adanez, J., A. Abad, F. Garcia-Labiano, P. Gayan, and F. Luis, *Progress in chemical-looping combustion and reforming technologies.* Progress in energy and combustion science, 2012. **38**(2): p. 215-282.

7. Thunman, H., M. Seemann, T. Berdugo Vilches, J. Maric, D. Pallares, H. Ström, G. Berndes, P. Knutsson, A. Larsson, C.J.E.S. Breitholtz, and Engineering, *Advanced biofuel production via gasification–lessons learned from 200 man-years of research activity with Chalmers' research gasifier and the GoBiGas demonstration plant.* 2018. **6**(1): p. 6-34.

8. Perejón, A., L.M. Romeo, Y. Lara, P. Lisbona, A. Martínez, and J.M.J.A.E. Valverde, *The Calcium-Looping technology for CO2 capture: On the important roles of energy integration and sorbent behavior.* 2016. **162**: p. 787-807.

9. Rydén, M., M. Hanning, A. Corcoran, and F. Lind, *Oxygen carrier aided combustion (OCAC) of wood chips in a semi-commercial circulating fluidized bed boiler using manganese ore as bed material.* Applied Sciences, 2016. **6**(11): p. 347.

10. Pardo, P., A. Deydier, Z. Anxionnaz-Minvielle, S. Rougé, M. Cabassud, and P. Cognet, *A review on high temperature thermochemical heat energy storage.* Renewable Sustainable Energy Reviews, 2014. **32**: p. 591-610.

11. Espatolero, S. and L.M. Romeo, *Optimization of oxygen-based CFBC technology with CO2 capture.* Energy Procedia, 2017. **114**: p. 581-588.

12. Mathekga, H., B. Oboirien, and B.C. North, *A review of oxy-fuel combustion in fluidized bed reactors.* International Journal of Energy Research, 2016. **40**(7): p. 878-902.

13. Myöhänen, K. and T. Hyppänen, *A three-dimensional model frame for modelling combustion and gasification in circulating fluidized bed furnaces.* International Journal of Chemical Reactor Engineering, 2011. **9**(1).

14. Johnsson, F. and B. Leckner. *Vertical distribution of solids in a CFB-furnace*. in *CONF-950522*. 1995. American Society of Mechanical Engineers, New York, NY (United States).

15. Werdermann, C.C., *Feststoffbewegung und Wärmeübergang in zirkulierenden Wirbelschichten von Kohlekraftwerken*. 1993: Shaker.

16. Couturier, M., B. Doucette, D. Stevens, S. Poolpol, and V. Razbin. *Temperature, gas concentration and solid mass flux profiles within a large circulating fluidized bed combustor*. in *11th International Conference on FBC, ASME*. 1991. Montreal.

17. Johnsson, F., W. Zhang, and B. Leckner. *Characteristics of the formation of particle wall-layers in CFB boilers*. in *Proceedings of the second international conference on multiphase flow*. 1995. The Japan Society of Multiphase Flow Nagoya.

18. Lafanechere, L. and L. Jestin, *Study of a circulating fluidized bed furnace behavior in order to scale it up to 600 MWe*. 1995, American Society of Mechanical Engineers, New York, NY (United States).

19. Leretaille, P., J. Werther, P. Briand, and D. Montat, *Modeling of hydrodynamics of large scale atmospheric circulating fluidized bed coal combustors*. 1999, Technical Univ. Hamburg-Harburg, Hamburg (DE).

20. Johansson, A., *Solids flow pattern in circulating fluidized-bed boilers*. 2005.

21. Mirek, P., *Influence of the model scale on hydrodynamic scaling in CFB Boilers.* Brazilian Journal of Chemical Engineering, 2016. **33**(4): p. 885-896.

22. Yang, H., G. Yue, X. Xiao, J. Lu, and Q. Liu, *1D modeling on the material balance in CFB boiler.* Chemical Engineering Science, 2005. **60**(20): p. 5603-5611.

23. Pallarès, D., *Fluidized Bed Combustion: Modeling and Mixing*. 2008, Chalmers University of Technology.

24. Myöhänen, K., *Modelling of combustion and sorbent reactions in three-dimensional flow environment of a circulating fluidized bed furnace.* Acta Universitatis Lappeenrantaensis, 2011.

25. Hannes, J.P., *Mathematical modelling of circulating fluidized bed combustion*. 1998.

26. Wischnewski, R., L. Ratschow, E.-U. Hartge, and J. Werther, *Reactive gas–solids flows in large volumes—3D modeling of industrial circulating fluidized bed combustors.* Particuology, 2010. **8**(1): p. 67-77.

27. Wen, C. and L. Chen, *Fluidized bed freeboard phenomena: entrainment and elutriation.* AIChE Journal, 1982. **28**(1): p. 117-128.

28. Kunii, D. and O. Levenspiel, *Entrainment of solids from fluidized beds I. Hold-up of solids in the freeboard II. Operation of fast fluidized beds.* Powder Technology, 1990. **61**(2): p. 193-206.

29. Johnsson, F., B. Leckner, and A. Vrager. *Solids flow pattern in the exit region of a CFB--Furnace influence of exit geometry*. in *CONF-990534*. 1999. Chalmers Univ. of Technology, Göteborg (SE).

30. Davidson, J., *Circulating fluidised bed hydrodynamics.* Powder Technology, 2000. **113**(3): p. 249-260.

31. Johnsson, F., A. Svensson, S. Andersson, and B. Leckner, *Fluidization Regimes in Boilers*, in *International Symposium of the Engineering Foundation*. 1995: Tours, France.

32. Svensson, A., F. Johnsson, and B. Leckner, *Fluidization regimes in non-slugging fluidized beds: the influence of pressure drop across the air distributor.* Powder Technology, 1996. **86**(3): p. 299-312.

33. Svensson, A., F. Johnsson, and B. Leckner, *Bottom bed regimes in a circulating fluidized bed boiler.* International Journal of Multiphase Flow, 1996. **22**(6): p. 1187-1204.

34. Kunii, D. and O. Levenspiel, *Fluidization engineering.* 1991.

35. Johansson, A., F. Johnsson, and B. Leckner, *Solids back-mixing in CFB boilers.* Chemical Engineering Science, 2007. **62**(1-2): p. 561-573.

36. Gayan, P., J. Adanez, F. Luis, F. García-Labiano, A. Cabanillas, A. Bahillo, M. Aho, and K. Veijonen, *Circulating fluidised bed co-combustion of coal and biomass.* Fuel, 2004. **83**(3): p. 277-286.

37. Pallares, D. and F. Johnsson, *Macroscopic modelling of fluid dynamics in large-scale circulating fluidized beds.* Progress in Energy Combustion Science, 2006. **32**(5-6): p. 539-569.

38. Löffler, G., S. Kaiser, K. Bosch, and H. Hofbauer, *Hydrodynamics of a dual fluidized-bed gasifier—Part I: simulation of a riser with gas injection and diffuser.* Chemical Engineering Science, 2003. **58**(18): p. 4197-4213.

39. Adanez, J., P. Gayan, L. De Diego, F. Garcia-Labiano, and A. Abad, *Combustion of wood chips in a CFBC. Modeling and validation.* Industrial engineering chemistry research, 2003. **42**(5): p. 987-999.

40. Gómez-Barea, A. and B. Leckner, *Modeling of biomass gasification in fluidized bed.* Progress in Energy Combustion Science, 2010. **36**(4): p. 444-509.

41. Lyngfelt, A. and B. Leckner, *A 1000 MWth boiler for chemical-looping combustion of solid fuels–Discussion of design and costs.* Applied Energy, 2015. **157**: p. 475-487.

42. Gómez-Barea, A. and B. Leckner, *Estimation of gas composition and char conversion in a fluidized bed biomass gasifier.* Fuel, 2013. **107**: p. 419-431.

43. Karlsson, T., X. Liu, D. Pallarès, and F. Johnsson, *Solids circulation in circulating fluidized beds with low riser aspect ratio and varying total solids inventory.* Powder Technology, 2017. **316**: p. 670-676.

44. Djerf, T., D. Pallarès, and F. Johnsson, *Bottom-bed fluid dynamics–Influence on solids entrainment.* Fuel Processing Technology, 2018. **173**: p. 112-118.

45. Zhang, W., F. Johnsson, and B. Leckner, *Fluid-dynamic boundary layers in CFB boilers.* Chemical Engineering Science, 1995. **50**(2): p. 201-210.

46. Edvardsson, E., L.-E. Åmand, H. Thunman, B. Leckner, and F. Johnsson. *Measuring the external solids flux in a CFB boiler*. in *Proceedings 19th FBC Conferance, May 21-24, Vienna Austria*. 2006.

47. Werther, J. *Fluid mechanics of large-scale CFB units*. in *Proc. 4th Int. CFB Conference*. 1993.

48. Van der Meer, E., R. Thorpe, and J. Davidson, *Flow patterns in the square cross-section riser of a circulating fluidised bed and the effect of riser exit design.* Chemical Engineering Science, 2000. **55**(19): p. 4079-4099.

49. Senior, R.C. and C. Brereton, *Modelling of circulating fluidised-bed solids flow and distribution.* Chemical Engineering Science, 1992. **47**(2): p. 281-296.

50. Yue, G., J. Lu, H. Zhang, H. Yang, J. Zhang, Q. Liu, Z. Li, E. Joos, and P. Jaud. *Design theory of circulating fluidized bed boilers*. in *18th International Conference on Fluidized Bed Combustion*. 2005. American Society of Mechanical Engineers.

51. Glicksman, L.R., *Scaling relationships for fluidized beds.* Chemical Engineering Science, 1984. **39**(9): p. 1373-1379.

52. Markström, P. and A. Lyngfelt, *Designing and operating a cold-flow model of a 100 kW chemical-looping combustor.* Powder Technology, 2012. **222**: p. 182-192.

53. Glicksman, L., M. Hyre, and P. Farrell, *Dynamic similarity in fluidization.* International Journal of Multiphase Flow, 1994. **20**: p. 331-386.

54. Horio, M., H. Ishii, Y. Kobukai, and N. Yamanishi, *A scaling law for circulating fluidized beds.* Journal of Chemical Engineering of Japan, 1989. **22**(6): p. 587-592.

55. Glicksman, L., M. Hyre, and K. Woloshun, *Simplified scaling relationships for fluidized beds.* Powder Technology, 1993. **77**(2): p. 177-199.

56. Van der Meer, E., R. Thorpe, and J. Davidson, *Dimensionless groups for practicable similarity of circulating fluidised beds.* Chemical Engineering Science, 1999. **54**(22): p. 5369-5376.

57. Sette, E., D. Pallarès, and F. Johnsson, *Experimental quantification of lateral mixing of fuels in fluid-dynamically down-scaled bubbling fluidized beds.* Applied Energy, 2014. **136**: p. 671-681.

58. Schöny, G., E. Zehetner, J. Fuchs, T. Pröll, G. Sprachmann, and H. Hofbauer, *Design of a bench scale unit for continuous CO2 capture via temperature swing adsorption—Fluid-dynamic feasibility study.* Chemical Engineering Research Design, 2016. **106**: p. 155-167.

59. Sasic, S., F. Johnsson, and B. Leckner, *Interaction between a fluidized bed and its air-supply system: Some observations.* Industrial & Engineering Chemistry Research, 2004. **43**(18): p. 5730-5737.

60. Leckner, B., P. Szentannai, and F. Winter, *Scale-up of fluidized-bed combustion–A review.* Fuel, 2011. **90**(10): p. 2951-2964.

61. Johnsson, F., R. Zijerveld, J.v. Schouten, C. Van den Bleek, and B. Leckner, *Characterization of fluidization regimes by time-series analysis of pressure fluctuations.* International journal of multiphase flow, 2000. **26**(4): p. 663-715.